Acta Biomaterialia 121 (2021) 41–67

Contents lists available at ScienceDirect

Acta Biomaterialia

journal homepage: www.elsevier.com/locate/actbio

Review article

Structural and mechanical properties of fish scales for the bio-inspired design of flexible body armors: A review

Prashant Rawat[a,b], Deju Zhu[a,b,*], Md Zillur Rahman[c], Francois Barthelat[d,*]

[a] Key Laboratory for Green & Advanced Civil Engineering Materials and Application Technology of Hunan Province, College of Civil Engineering, Hunan University, Changsha 410082, China
[b] International Science Innovation Collaboration Base for Green & Advanced Civil Engineering Materials of Hunan Province, Hunan University, Changsha 410082, China
[c] Department of Industrial Engineering, BGMEA University of Fashion and Technology, Dhaka 1230, Bangladesh
[d] Department of Mechanical Engineering, University of Colorado, 427 UCB, 1111 Engineering Dr, Boulder, CO 80309, United States

ARTICLE INFO

Article history:
Received 17 September 2020
Revised 17 November 2020
Accepted 1 December 2020
Available online 5 December 2020

Keywords:
Fish scales
Hierarchal structures
Mechanical properties
Natural armor
Flexible body armor

ABSTRACT

Natural protection offered to living beings is the result of millions of years of biological revolution. The protections provided in fishes, armadillos, and turtles by unique hierarchal designs help them to survive in surrounding environments. Natural armors offer protections with outstanding mechanical properties, such as high penetration resistance and toughness to weight ratio. The mechanical properties are not the only key features that make scales unique; they are also highly flexible and breathable. In this study, we aim to review the structural and mechanical characteristics of the scales from *ray-finned* or *teleost* fishes, which can be used for new bio-inspired armor designs. It is also essential to consider the hierarchical structure of extinct and existing natural armors. The basic characteristics, as mentioned above, are the foundation for developing high-performance, well-structured flexible natural armors. Furthermore, the present review justifies the importance of interaction between toughness, hardness, and deformability in well-engineered bio-inspired body armor. At last, some suggestions are proposed for the design and fabrication of new bio-inspired flexible body armors.

Statement of significance

In this study, we aim to review the structural and mechanical characteristics of the scales from *ray-finned* or *teleost* fishes, which can be used for new bio-inspired armor designs. It is also important to consider the hierarchical structure of extinct and existing natural armors. The basic characteristics, as mentioned above, are the foundation for developing high performance, well-structured flexible natural armors. Furthermore, the present review justifies the importance of interaction between toughness, hardness, and deformability in well-engineered bio-inspired body armor. At last, some suggestions are proposed for the design and fabrication of new bio-inspired flexible body armors.

1. Introduction

Many organisms live with body armor for protection against threats. The existence of armors (bony plate, shells, scales, and osteoderms) in the animal world is for a long time, such as 419-million-year-old Placoderm fossil in China and 155~150-million-year-old Stegosaurus in America and Portugal. Natural armors can generally be classified into two types — scales and osteoderms. Scales can be seen in many fishes (e.g., *Arapaima gigas (dragonfish), Mugil cephalus, Cyprinus carpio, Carassius auratus, etc.*). In contrast, Osteoderms (i.e., bony elements form tough skin structures) are found in reptiles (crocodiles, alligators, and turtles). Mammals (armadillo) also have armors that are sufficiently strong to prevent penetration [1]. The thickness of natural armors may vary from fractions of millimeters to 100 mm (e.g., scales of small fishes to dinosaurs) of thick plates. Despite the size variation, the critical factor is the flexibility offered by these armors [2]. The ratio of armor plate to animal size can be termed as armor flexibility. Various attributes of armors act as inspiration for designing synthetic lightweight, flexible, and high toughness armors [3,4].

* Corresponding authors.
E-mail addresses: dzhu@hnu.edu.cn (D. Zhu), francois.barthelat@colorado.edu (F. Barthelat).

https://doi.org/10.1016/j.actbio.2020.12.003
1742-7061/

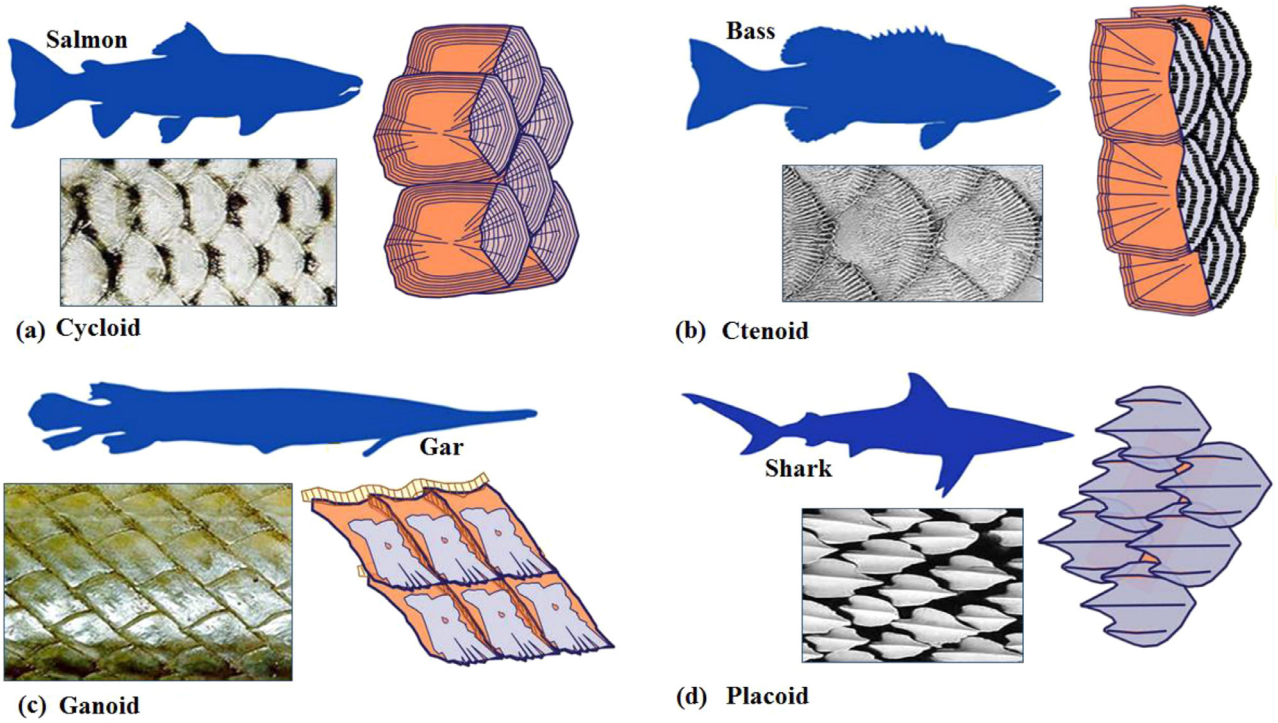

Fig. 1. The arrangement, schematics of overlapping with examples of (a) Cycloid, (b) Ctenoid, (c) Ganoid, and (d) Placoid fish scale [2].

Fish scales can be four major types: (i) cycloid, (ii) ctenoid, (iii) ganoid, and (iv) placoid [5]. Different types of fish scales, along with overlapping patterns, are shown in Fig. 1. Cycloid scales have concentric "ring"-like acellular structures, whereas ctenoid scales carry "comb"-like structures at the protective edges. The concentric rings represent the annual growth of a fish, as similar to the tree rings (dendrochronology — tree ring dating method). A thick bony structure at the top side with a ganoine or enamel made (inorganic substance) surface layer is the unique feature of ganoid scales. These scales have a rhomboid shape with articulating "peg and socket joints" between adjacent scales. In contrast, placoid scales show "tooth"-like structures known as dermal denticles. Vitrodentine (enamel-like substance) covers the outer layer of placoid scales, which cannot grow in size but increase in number with time [2]. Additionally, one more type of scale named "cosmoid" [5,6] was found in the earliest (fossil) fishes. These fossil fishes were armed with bulky and bony scales that offered them effective protection from predators [7].

Fish scales have become more flexible, lightweight (compared with integumental skeleton), and often transparent (e.g., *Juvenile surgeonfish*) throughout its natural evolution. The thin and flexible "teleost" scale enhances the speed and swimming maneuverability of modern fish [8]. The thin, transparent, and collagen-based "plate"-like elasmoid scales (i.e., cycloid and ctenoid) [9,10] offer improved hydrodynamic properties [11] and resistance to penetration.

Various testing methods have been developed over the past few decades for the mechanical and microstructural analyses of biological materials, including nacre [12], armadillo [11], and turtle. To the best of the authors' knowledge, the first mechanical testing on fish scales was performed by Ikoma et al. [13] in 2003. This study reported the ductility aspects in the fish scale, which significantly improve the mechanical characteristics due to its unique design. Since then, numerous studies have been performed on the mechanical behavior of fish scales and inspired structures derived from them. This review paper aims to detail the structures, mechanical behavior, and failure mechanisms of fish scales. Moreover, this review on the structure-property relationship can help in designing lightweight and flexible body armors.

2. Structure of teleost fish skin

The teleost fish skin consists of two layers — the inner one is called "dermis," and the outer one is known as "epidermis" [8,14,15]. Each scale is separately embedded in the fish skin pocket (see Fig. 2) so that pocket can spontaneously lose its scale whenever needed. In general, the epidermis and the outer surface of fish skins have unique features that make them suitable for penetration-resistant designs in the marine environment. The main constituents of fish scales are calcium-deficient hydroxyapatite (HAP) and extracellular matrix (type I collagen fibers). Both constituents form a high ordered 3D structure [9,16].

Several epidermis layers cover the surface of fish scales, as shown in Fig. 3a. These layers are intricately patterned (Fig. 3b-c), resulting in an appropriate design of natural armor for the fish [14]. Fig. 3d-g demonstrate the variation in scale morphologies for four fishes from different regions (freshwater to seawater) [17]. The natural structures or structural orientations of the hard scale surface are attributed to the high resistance to wear or penetration [18]. The entire epidermis, which comprises continuous micro-ridges and short segments of micro-ridges, acts as a natural mechanical defense system for fish protection.

The external layer composes of randomly oriented mineralised collagen fibers and mineral deposits (known as "osseous"). In the internal layer, coaligned collagen fibers form a "plywood"-like structures, which are orthogonally arranged at different angles, and the orientation of fiber angle depends on the fish scale [19]. The cross-sections of typical fish scales are shown in Fig. 4, which demonstrates the outer and internal "collagen" layers in a fish scale. Fig. 4a and c illustrate the optical micrographs of the

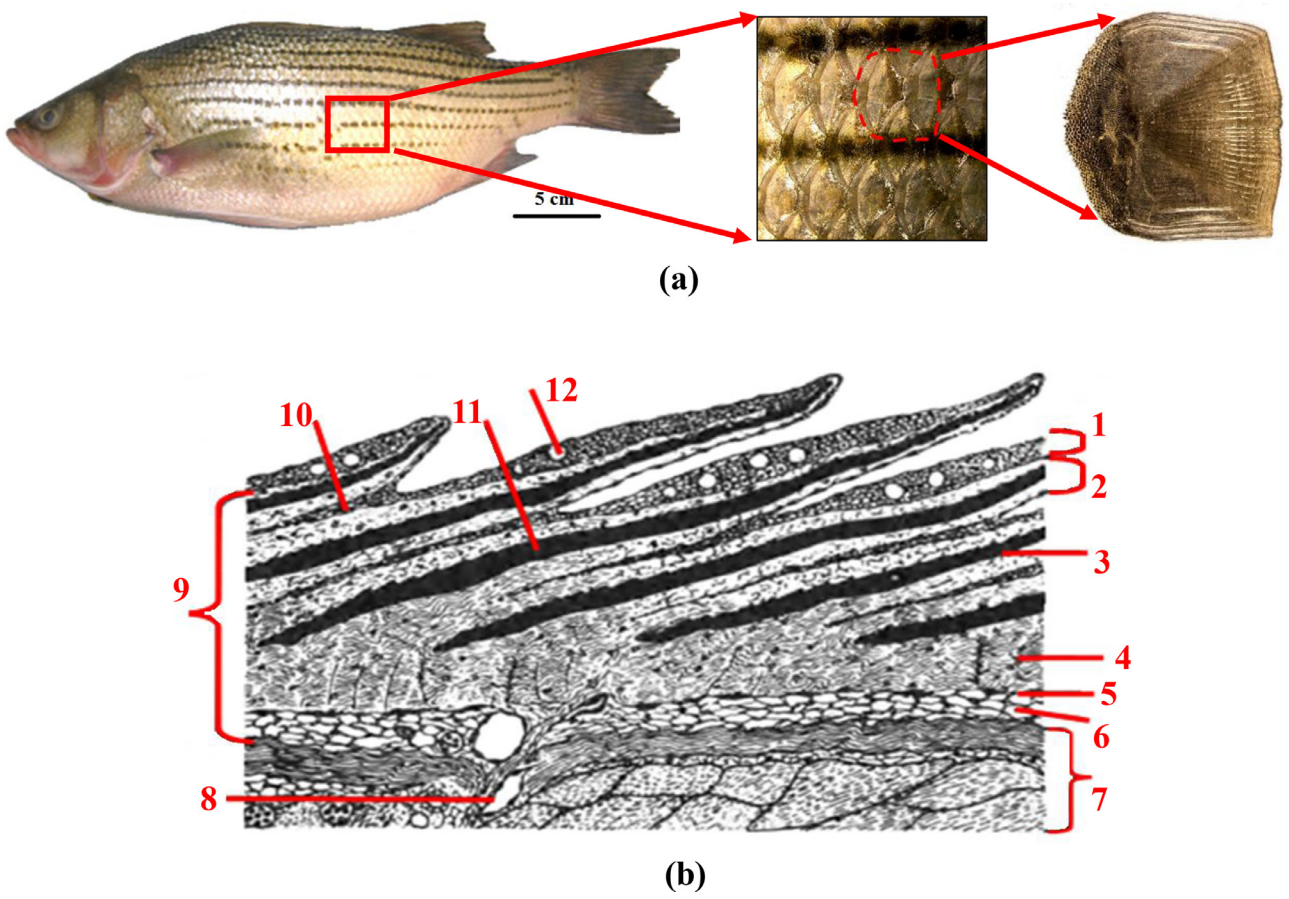

Fig. 2. (a) The hierarchical structure of Morone saxatilis, and (b) Skin of yellow perch: *(1) epidermis, (2) dermis, (3) scales, (4) dense fibrous tissue, (5) pigment cells, (6) subcutis, (7) muscle, (8) septum, (9) dermis, (10) pigment cells, (11) scales, and (12) mucous cell* [5]. (For interpretation of the references to color in this figure legend, the reader is referred to the web version of this article.)

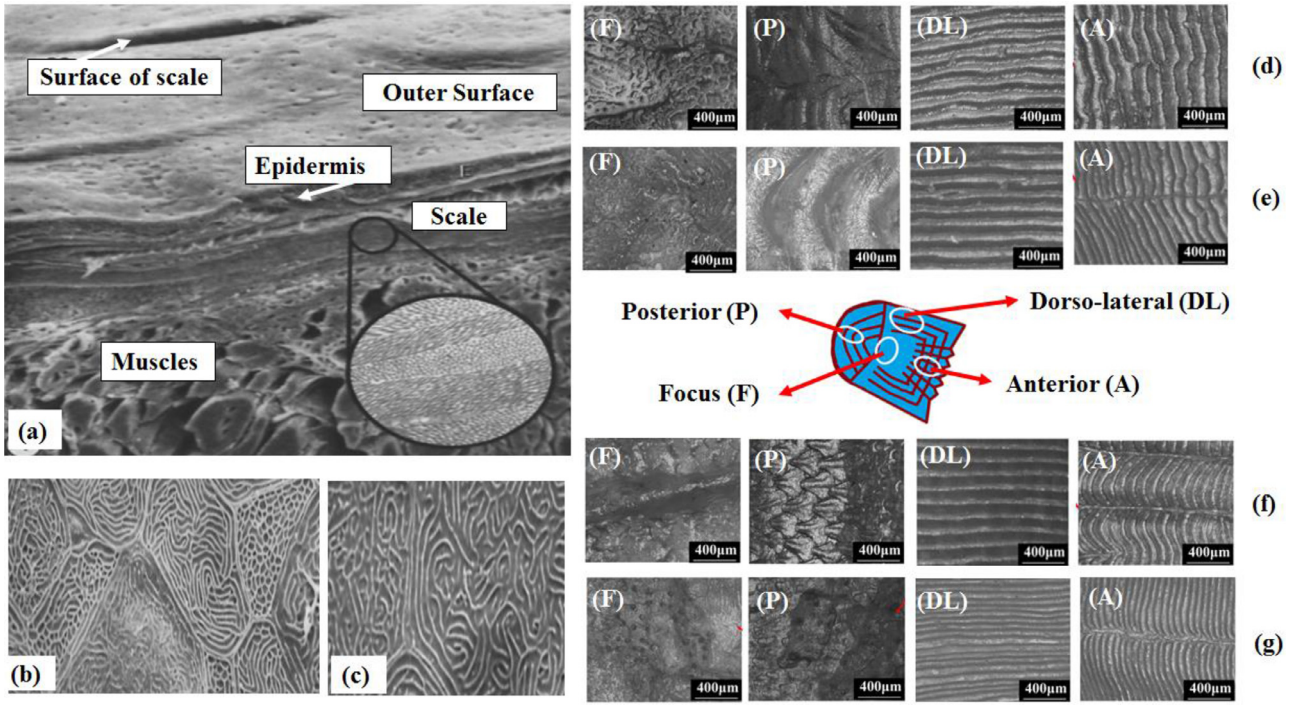

Fig. 3. (a) The outer surface, the cryostat-faced edge of *coho-salmon* skin, muscle and Epidermis, (b-c) continuous micro-ridges and short segments of micro-ridges form a fingerprint pattern over the cell surface [14], the surface morphology of scales obtained from (d) *Cyprinus carpio*, (e) *Carassius auratus*, (f) *Mugil cephalus*, and (g) *Pristipomoides sieboldii* [17].

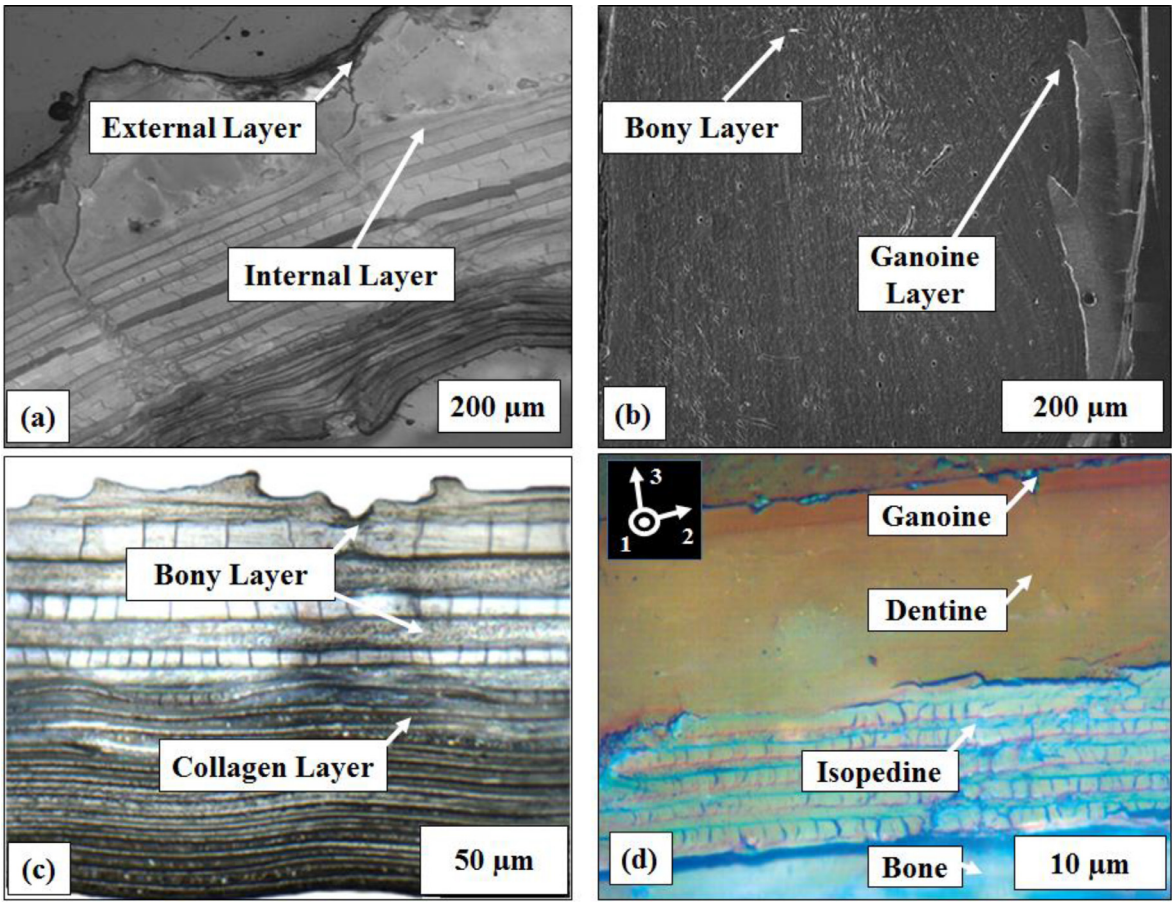

Fig. 4. The cross-sections of different fish scales: (a) *Arapaima gigas* [22], (b) *Atractosteus spatula* [20], (c) *Striped bass* [7], and (d) *Polypterus senegalus* [23].

internal and external layers of scales of *Arapaima gigas* and *Striped bass*, respectively. The external layers with a corrugated surface indicate the rigid structures of the scale; the internal layers are soft collagen fibers (Fig. 4). Fig. 4b shows a scanning electron microscopy (SEM) image of an *Atractosteus spatula* scale (transverse section) and differentiates lamellar bone, diffuse bone, and ganoine layer [20]. The variation in the cross-sectional analysis of scale components indicates the importance of understanding the hierarchical structure for designing a bioinspired armor. Fig. 4d shows four layers (organic and inorganic) of a *Polypterus senegalus* fish scale, and these layers form a nanocomposite design contributing to outstanding mechanical properties for protecting against penetration [21].

The collagen fiber laminates are stacked with angles of 60°–70° with one another, thereby creating "Bouligand"-type [24] orientations which look like a "helicoid" [2], as shown in Fig. 5. The angles of collagen fibers vary from species to species [25,26]. A single collagen fiber has a diameter of 1 µm with a total collagen layer thickness of approximately 100 µm. The thicknesses of bony and collagen layers of striped bass is roughly the same (i.e., 100 µm in the selected fishes), and the HAP mass fraction and density of collagen are 46% and 3.17 × 103 kg.m^{-3}, respectively [7]. The outer layer of a fish scale has more minerals than the internal collagen layer [25,27].

The arrangement of scales over the fish body is important to consider from the perspective of the strain-stiffing effect. Zhu et al. [7] demonstrated that the arrangement pattern of the fish scale could significantly improve the penetration strength. During swimming, when the fish body bends, it results in rotation and deformation of the adjacent scales. The adjacent scales with increased contact side develop "strain-stiffing" properties due to the rearrangement of scales [28]. The rearrangement helps fishes in two aspects; firstly, it improves the drag force during swimming [29,30] and then offers high penetration strength. Fig. 6a-b illustrate the importance of scale deformation mechanism when well-arranged fish scales (over the fish body) are subject to penetration load. The rearrangement of scales forms a stiff barrier and also redistributes the applied force. However, in the absence of the scale arrangement, the applied force focuses at a point which is not desirable as it may cause severe damage under the attacking situation. Therefore, the rearrangement of scales is an effective protection mechanism in teleost fishes.

3. Mechanical properties and structures of teleost fish scales

The Young's modulus of engineering materials as a function of density is exhibited in Fig. 7a [32]. A new lightweight bioinspired material with superior mechanical properties can be developed using a combination of engineering materials and fish scales. The seven inspirational features of biological materials (e.g., fish scales) described by the Arzt heptahedron [33–35] are as follows (Fig. 7b): (i) self-assembly, (ii) self-healing, (iii) evolutionary and environmental constraints, (iv) the importance of hydration, (v) mild synthesis conditions, (vi) multi-functionality, and (vii) the hierarchy of structure at nano-, micro-, meso-, and macro-levels.

From a technical point of view, the fish skin (with scales) can act as an inspiration for designing new engineering materials or structures [35] with high mechanical performance under different

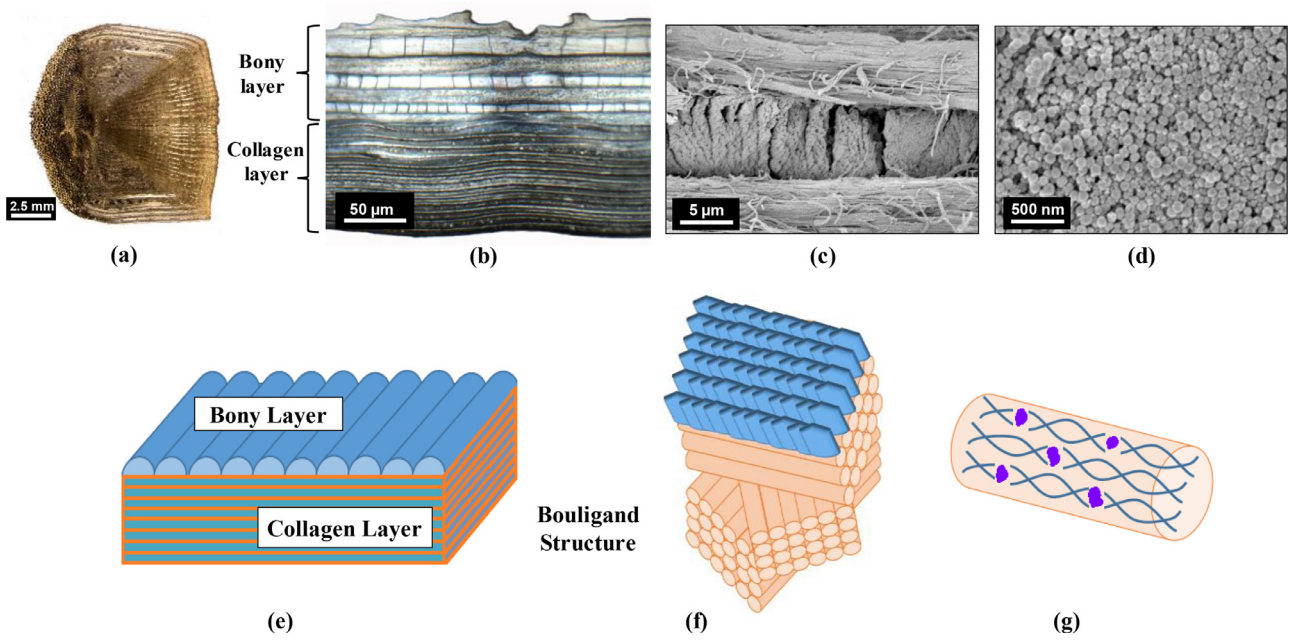

Fig. 5. The hierarchical structure of *striped bass* scale: (a) single scale, (b) cross-sectional view of the single scale with bony and collagen layers, (c) cross-ply structure of collagen fibers, (d) collagen fibrils [7], and (e) schematic representations of bony and collagen layers in which (f) collagen fibers are arranged in the Bouligand pattern, and (g) constituents of a single fibril with HAP nanoparticles [27].

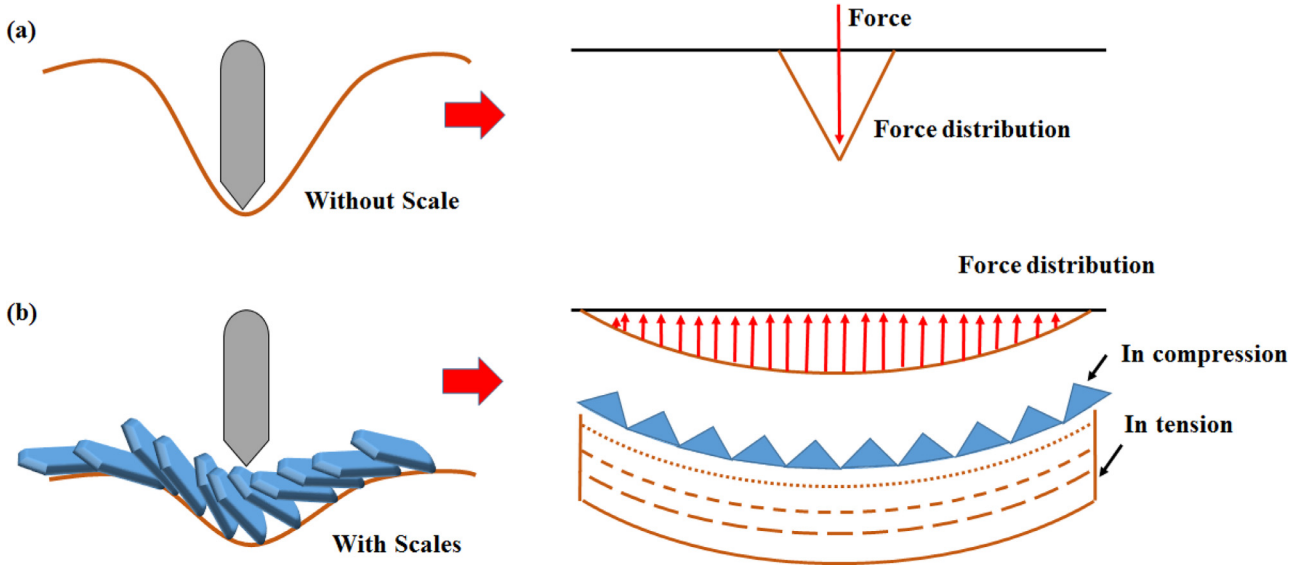

Fig. 6. Schematics of deformation mechanisms for fish skins under penetration test, and 2D representation of force diagram with force-distribution-status in fish skin: (a) without scales, and (b) with scales in which scales rearrange themselves during the penetration to distribute force throughout the skin [31].

loading conditions. Fish skin has a hierarchical structure of scales arrangement, which makes it difficult to penetrate by a predator [2,3]. The current form of fish skin or other natural hierarchical structure is a result of millions of years' evolution and offers amazing combinations of various constituents [36–38]. The building blocks or constituents of these hierarchical structures (fish, bone, and nacre) display unique and attractive combinations of mechanical strength and toughness [12,39]. For example, the external ganoine layer (see Fig. 4d) with rich mineral zones protects the fish from predators. The inner collagen layer with collagenous fibers (see Fig. 4c) acts as a soft buffer for fish scales, which protects fish skin from the direct impact of the attacker's tooth. Zhu et al. [17] compared the surface morphologies, hierarchical structures, and mechanical properties of four types of scales of fishes living in freshwater and seawater. The results showed that structural arrangement variations lead to changes in mechanical properties in fish scales from different regions. Differences in spiral angles in fish scales from New Zealand (with varying water regions) are shown in Fig. 8a-d. Fishes typically develop or modify their scale structures as per the requirements of the surrounding environments and defense priorities [40]. Therefore, without proper knowledge of surface morphologies, hierarchical structures, and

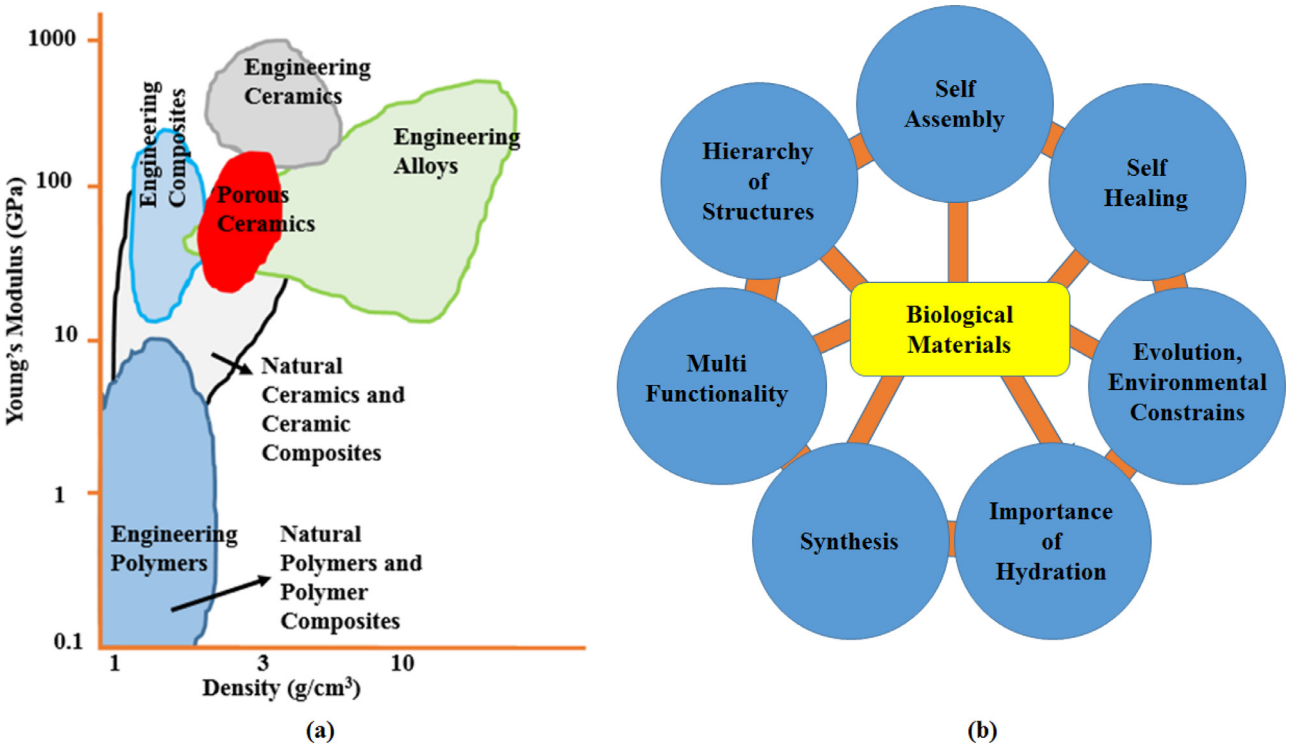

Fig. 7. (a) Young's modulus as a function of density for various materials [32], and (b) seven unique features of biological materials described by the classic Arzt heptahedron [33,34,42].

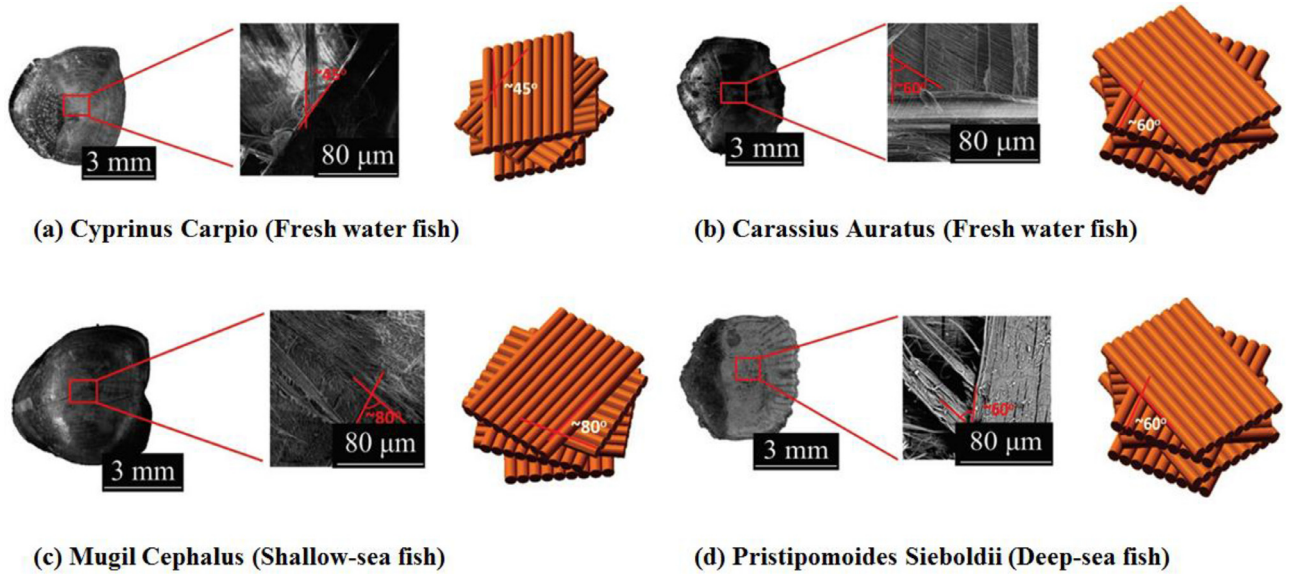

Fig. 8. The variations in the spiral angles of collagen lamellae for the teleost fish scales collected from different water regions in New Zealand [17].

mechanical properties [41], including strength, stiffness, and fracture toughness, the development of bio-inspired flexible armors for human protection is not feasible.

3.1. Tensile properties of teleost fish scales

The tensile test is one of the basic mechanical tests to measure the strength and stiffness (Young's modulus) of materials. Ikoma et al. [13] carried out tensile testing on fish scales (*Pagrus major*). They revealed that the behavior of the fish scale in tension was initially linear, followed by plastic yielding before fracture. This yielding is a result of collagen fiber sliding and the pullout of individual fibers, as depicted in Fig. 9. The mechanical properties, such as Young's modulus and tensile strength of *Pagrus major* scales, are determined as 2.2 ± 0.3 GPa and 93 ± 1.8 MPa, respectively. However, this study inspired the researchers to investigate the mechanical properties of fish scales and its interrelation with scale location (over the fish body), presence of mineral content, and fiber orientation.

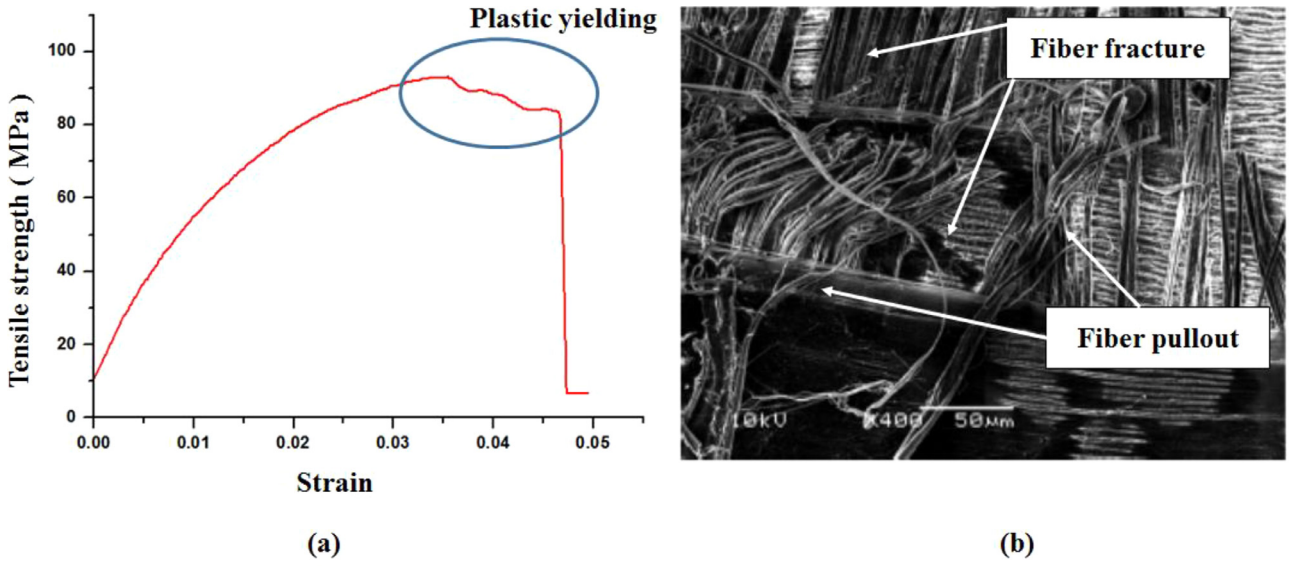

Fig. 9. (a) Typical tensile stress-strain curve of *Pagrus major* scales and its plastic yielding behavior, and (b) SEM image of the fractured sample showing breakage and pullout of collagen fibers [13].

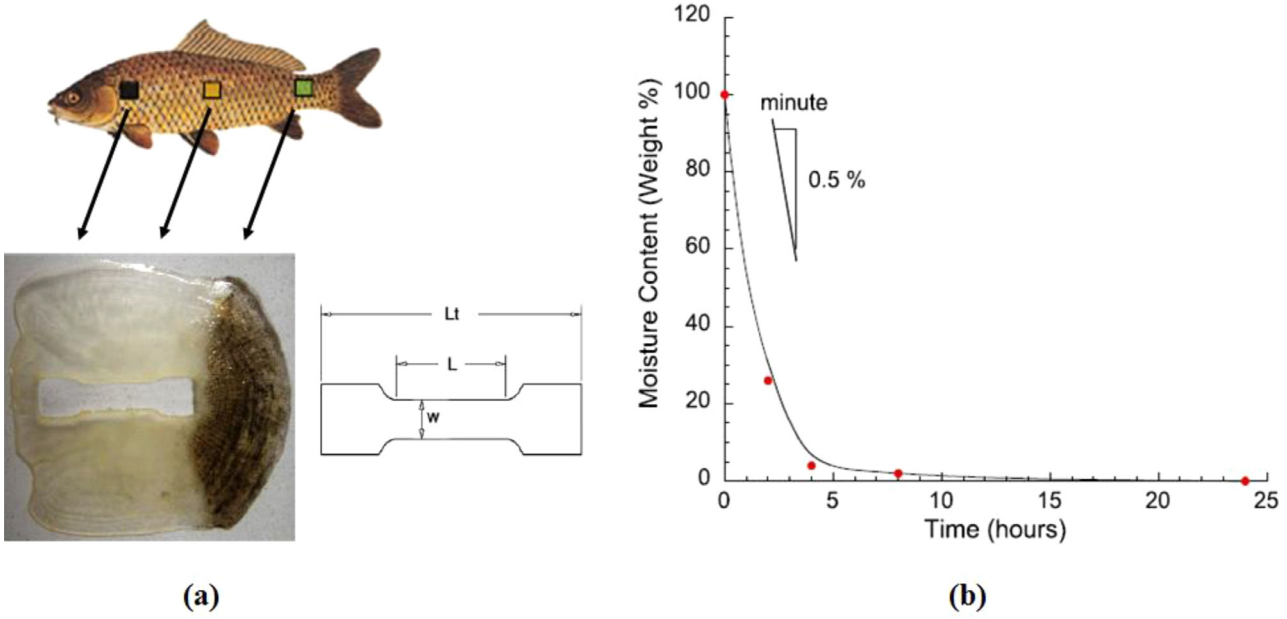

Fig. 10. (a) Anatomical positions (head, middle, and tail) of the sample preparation and specifications of the sample (Lt = 16 mm, L = 7 mm, and w = 3 mm), and (b) Moisture content versus drying time [45].

Torres et al. [43] performed mechanical testing on *A. gigas* scales under dry and wet conditions. This study confirmed that individual fish scales behave similar to a composite laminate under different loading conditions. They observed successive failure modes during the tensile testing; as a result, Young's modulus and tensile strength decreased after soaking scales in distilled water for four days. The tensile strength (53.86 ± 8.36 MPa) of dry samples was higher than that (22.26 ± 3.94 MPa) of wet samples. An important finding of this analysis was only 18% variation in strain under both conditions, while the stress varied by nearly 60%. Lin et al. [44] tested the air-dried and rehydrated scales of *A. gigas* after four days of distilled water treatment, and scales were extracted from the lateral part of the fish body. Tensile tests revealed that the tensile strength (46.7 ± 4.6 MPa) for dry samples was significantly higher than that (25.2 ± 7.3 MPa) for rehydrated samples. The linearity of the stress-strain curves of the tested scales was influenced considerably by hydration conditions. However, the failure of the samples was similar to the failure of laminated composites with multiple peaks. Garrano et al. [45] investigated the mechanical behavior of fish scales of *Cyprinus carpio* from different anatomical locations (head, body, and tail) as a function of moisture content in scales. They found that the mechanical behavior of fish scale is highly dependent on the anatomical locations. This study also observed that anatomical locations influence the mechanical properties of the scales (Fig. 10a). The loss of moisture content during the dehydration process depends on the drying time. A higher amount of moisture loss occurred within the first four hours of dehydration; thus, the moisture loss in scale is de-

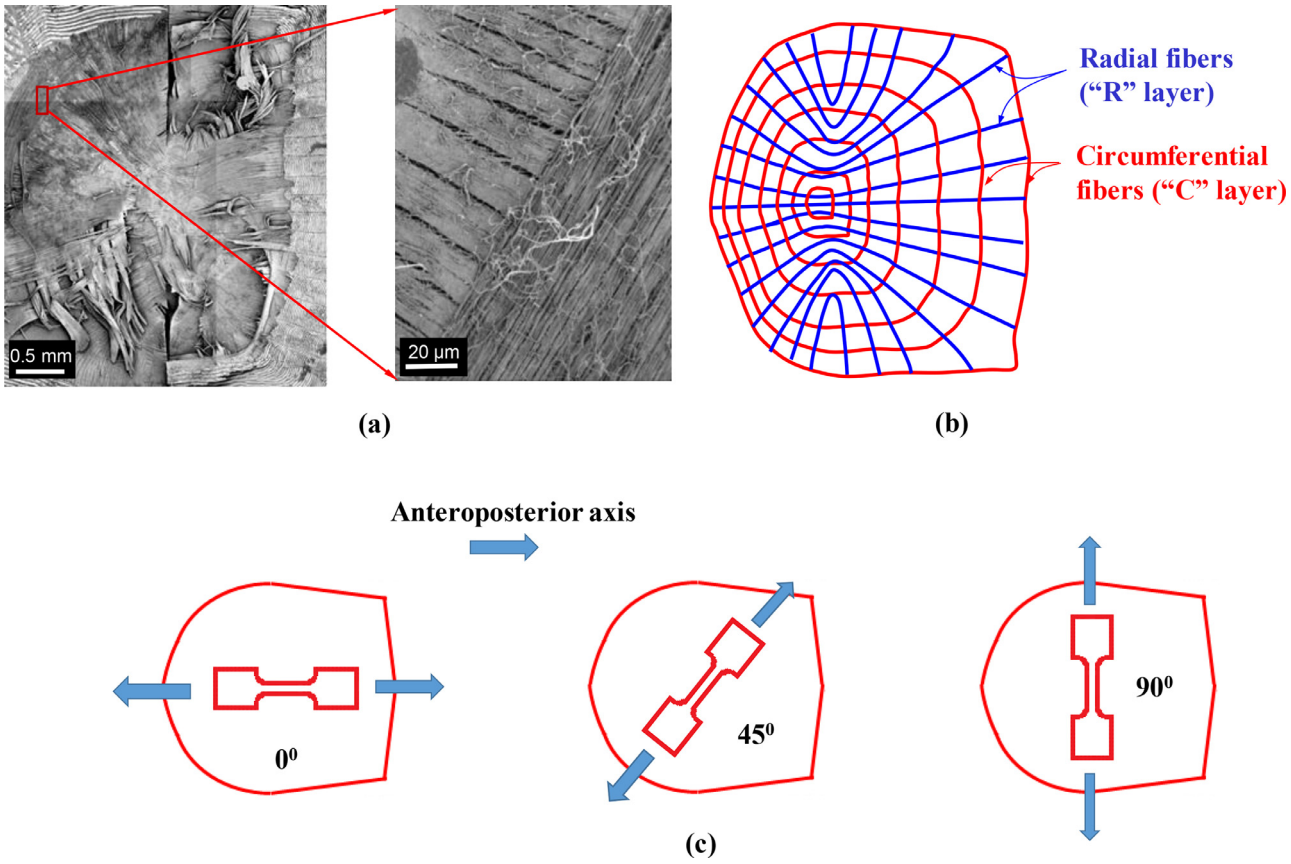

Fig. 11. (a) The arrangement of collagen fibrils in *Striped bass* scale, (b) Fiber pattern "R" and "C" layers in the scale, and (c) samples with different orientations for tensile testing [7].

pendent on the hydration time (Fig. 10b). The strength and elastic modulus of head scales were nearly twice than those of tail scales. Importantly, for the dehydrated samples, no significant difference in mechanical strength was observed among scales taken from any position (i.e., from head to tail).

The arrangement of collagen fibrils (see Fig. 11) and the tensile strength of the striped bass scale (on the whole scale and the collagen layer) were examined by Zhu et al. [7]. They found that the angular variations affect mechanical properties. The tensile strength and Young's modulus variations lie in the range of 30 to 50 MPa and 600 to 850 MPa, respectively, for fish scales along 0°, 45°, and 90° from the longitudinal axis (anteroposterior axis) of the fish. The ultimate strain is the same for the samples with or without the bony layer (only collagen fibers). This finding implied that the behavior of collagen fiber is mainly controlled by the stretching of straight, individual collagen fibers.

For identifying the possibilities of bio-inspired designs for flexible protective armor, the structural and mechanical characteristics of arapaima (*Arapaima gigas*) scales (Fig.s 12a-c) were investigated [31]. The study concluded that the elasmoid scales consist of HAP and type-I collagen fibers, and the aspect ratio of the scale is approximately 50. The outer layer is highly mineralised, whereas the mineral content is low in the inner layer. The inner layer or a combination of lamellae (with the thickness of 45–60 μm) was arranged at different orientations (e.g., twisted plywood and Bouligand structures). Interestingly, the fibrils of the lamellae were varied ($\alpha 1$ = 86.70, $\alpha 2$ = –34.50, $\alpha 3$ = –69.20, and $\alpha 4$ = 66.90), which proved that orientations of lamellae vary throughout the sublayer section in *A. gigas*. The shape of collagen fibers was cylindrical, and the packing of fibers in each layer was visible, as observed in TEM and AFM micrographs. The Young's modulus and tensile strength (for the entire scale and collagen layer) of the longitudinal samples were higher than the transversely orientated samples (Fig. 12b-c). The ultimate tensile strengths of collagen layers in longitudinal and transverse directions (36.9 ± 7.4 MPa and 21.8 ± 2.4 MPa, respectively) were greater than that (23.6 ± 7.2 MPa and 14.2 ± 1.1 MPa, respectively) of the whole scale. The major failure modes of scales, as shown in Fig.s 12d-f, are as follows: (a) delamination of lamellae, (b) complete breakage of the outer layer, and (c) fracture of collagen fibers near the bony layer.

The tensile properties of *M. atlanticus* fish scales are position- (i.e., head, middle, and tail) and fiber orientation-dependent, as observed by several authors [46,47]. Notably, the higher mechanical properties in scales from the head region are due to the presence of a higher number of plies with the parallel sublayer-fiber direction. The mechanical features (e.g., tensile strength and toughness) of carp scales [47] are more compliant than other armors/tissues such as arapaima scales [44], human femur bone [48], bovine cortical bone [49], horn keratin [50], and rat-tail tendon [51]. In addition, the mechanical properties of fish scales of Asian carp depend on the loading strain rates from 10^{-4} to 10^{3} s^{-1}. Tensile tests with varying strain rates (for comparative analysis of elastic modulus) on Asian carp, Arapaima showed that the mechanical characteristics of scales are similar to human femur bone, horn, and rat tail tendon. Moreover, the fracture microstructure of damaged fish scales proved that scale's structure is more suitable for penetration loading as compared to tensile loading [47]. Zhu et al. [17] examined the mechanical properties of four different types of fish scales (see Fig. 3d-g) and concluded that the hierarchical struc-

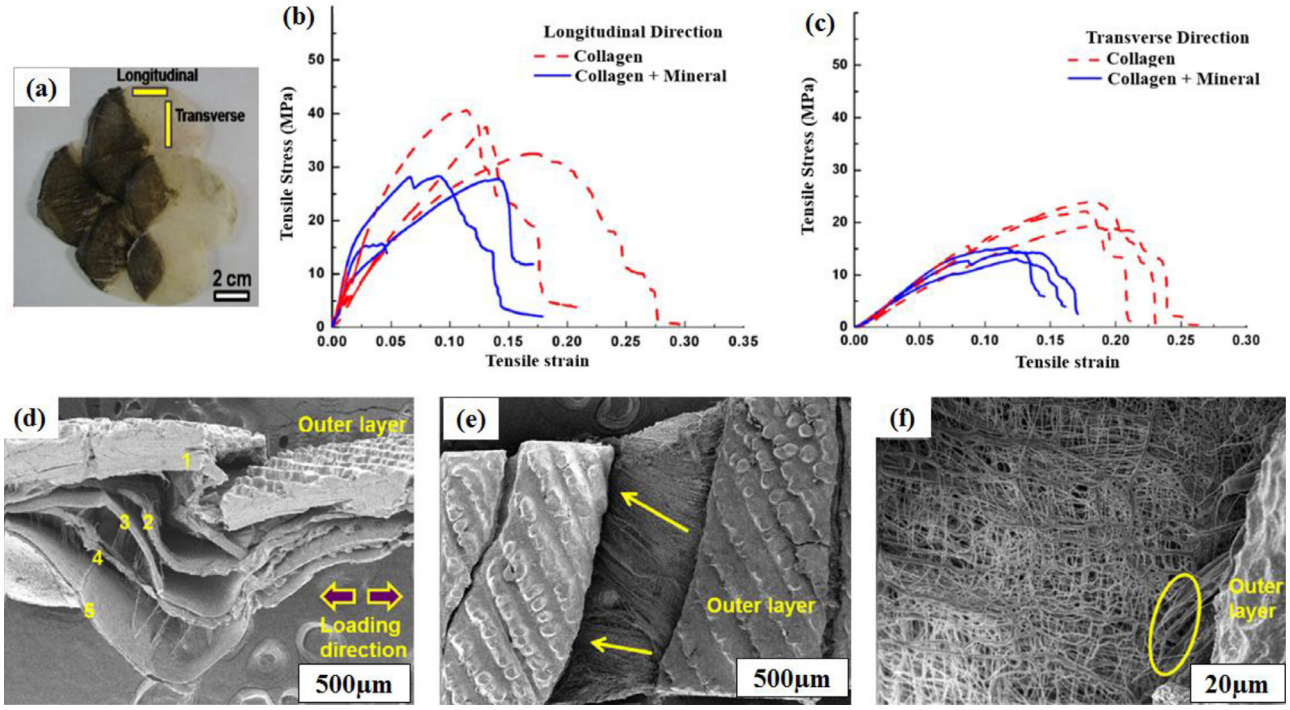

Fig. 12. (a) Overlapped scales of *Arapaima* fish showing longitudinal and transverse directions selected for mechanical testing, (b, c) Tensile stress-strain curves in longitudinal and transverse directions for collagen and collagen + mineral layers, respectively, (d) side view of fractured scale showing delamination of different layers, (e) top view of the fractured surface showing complete fracture of bony layer and exposed collagen fibers, and (f) the fracture of outer layer after tensile testing and the separation of collagen layers from the outer layer [31].

tures of scales significantly affect the mechanical properties. The variation in scale causes a change in strength (maximum strength in *Carassius auratus* scales) and toughness (maximum toughness in *Pristipomoides sieboldii* scales). Therefore, studying the mechanical behavior of a wide variety of fish scales is necessary to design and develop the bioinspired armors with optimum mechanical features (i.e., high strength and toughness).

3.2. Puncture and indentation properties of teleost fish scales

Skin and scales should protect the fish from predators' teeth [52,53] or a sharp object penetration [54]. The bite force of a *piranha* (weighing 1 kg) is equivalent to about 20 N [52]. During an attack, this bite force is concentrated over a small area of a single scale. Meyers et al. [52] identified the situation at a battle in Amazon between *arapaima* and *piranha*. They also performed a penetration test on the internal and external regions of *arapaima* scale using a real *piranha* tooth and compared the results with the test results stemmed from synthetic rubber and salmon meat (see Fig. 13). The finding infers an important aspect of developing bioinspired armors. A piranha tooth failed to penetrate the hard-mineral layer of the fish scale regardless of the complicated structure of the tooth. By contrast, internal collagen fibers or soft layers were entirely fractured by the tooth. However, a combination of strong and soft materials (e.g., fish scale) can be used to make a commendable design for the puncture resistance [7].

Understanding the basic fracture mechanisms involved during the complete penetration of a fish scale is essential to develop an armor inspired by fish skin structure. Zhu et al. [7] investigated the puncture process on the whole scales (Fig. 14a) of striped bass fish using a sharp steel needle ($R = 25$ μm). The load-displacement curves of fish scale, polycarbonate, polystyrene, and collagen are shown in Fig. 14b. The fish scale showed considerably better load response and resistance against puncture than the polymers. Sequences of puncture tests were also presented and divided into three stages, as follows (Fig. 15): (i) Stage I shows a linear region with increasing load; the bony layer of the scale carried this load. At the end of stage I, a slight drop in load was observed at 2 N owing to the initial fracture of the bony layer. (ii) During stage II, the load was carried by both bony and collagen layers. The load continuously increased until reaching the complete delamination of the bony layer with the formation of four "flaps", and the complete penetration of the bony layer happened at the end of this stage. (iii) At stage III, the needle started penetrating the collagen layer, and a continuous drop in load-carrying capacity was seen with the delamination between bony and collagen layers. Further investigations using an idealised puncture configuration showed that two forces resist the deflection of flaps; namely, (i) bending moment transmits through the ligament of the bony layer, and (ii) the intact collagen layer acts as a "retaining membrane" for the flaps.

Puncture tests on multiple overlapped fish scales [55] were also performed and found that the overlapping of three scales increases the puncture force by three times compared with a single scale. Fig. 16 depicts the experimental method adopted for puncture tests and the load-displacement curves for puncture tests of 1, 2, 3, 5, and 10 scales. The study demonstrated that the focus of the scale has the maximum puncture resistance due to its larger thickness compared to the other locations (e.g., posterior, anterior, ventro-lateral, and dorso-lateral) in the scale.

The puncture tests for different scale arrangements (see Fig. 17) such as stacked, staggered (natural) overlap, and rotated were performed by Zhu et al. [55]. There was no influence of various arrangements of scale on stiffness. The same penetration resistance and a slight difference in peak load were measured in the case of staggered overlap and rotated arrangements. Ghods et al. [47] analysed the dynamic responses at 0.5, 5, and 50 mm/s loading rates of fish scales from the head, middle, and tail regions and compared

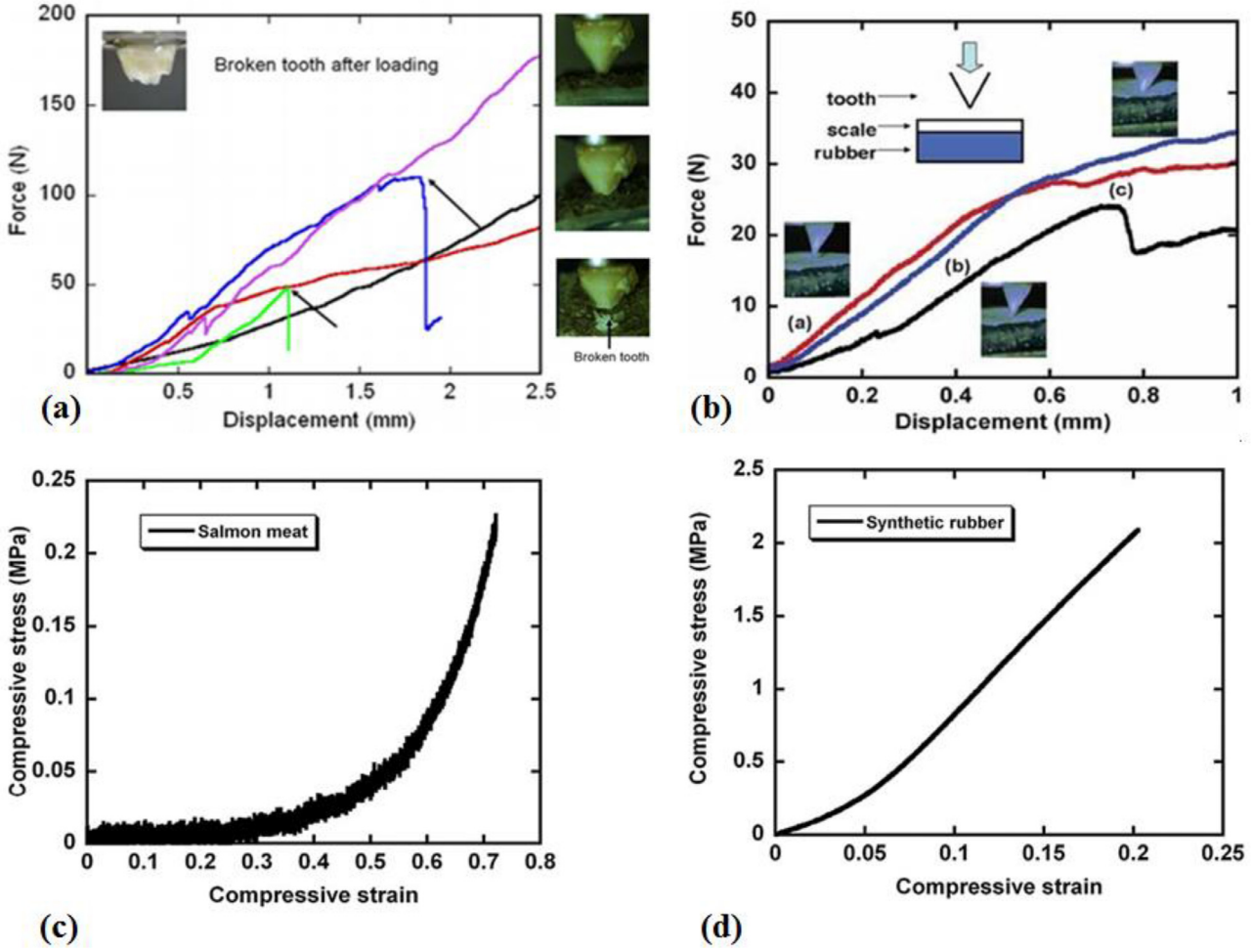

Fig. 13. Puncture testing on '*Arapaima*'s scale using *piranha* tooth: (a) external regions and (b) internal regions; compressive stress-strain curves for (c) salmon meat and (d) synthetic rubber [52].

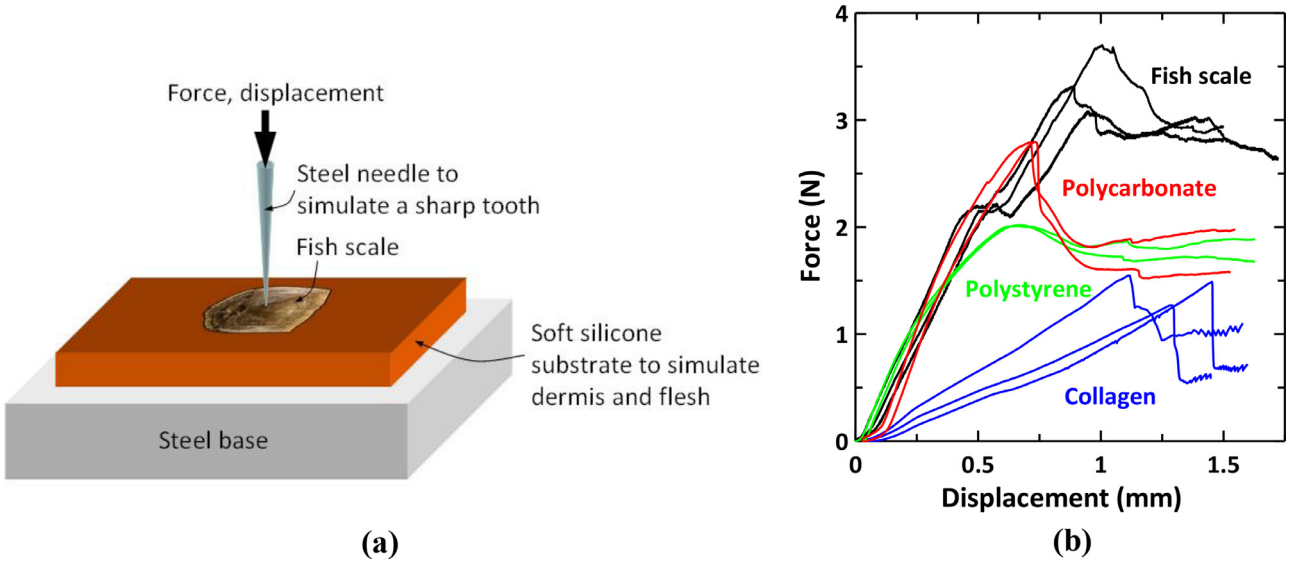

Fig. 14. (a) Puncture testing of striped bass scale with a steel needle and (b) puncture force versus displacement curves for various materials [7].

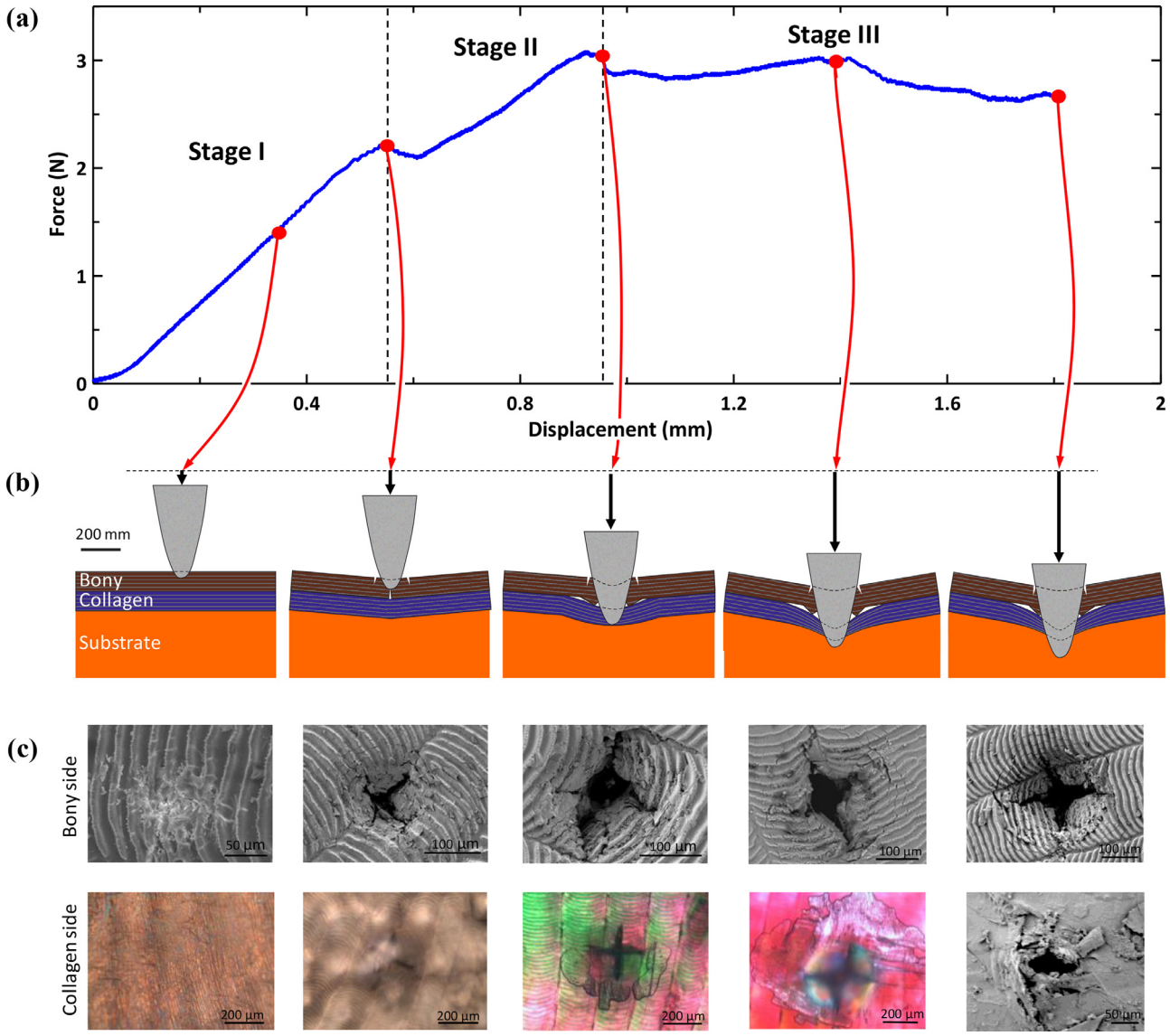

Fig. 15. (a) Force versus displacement curve showing the fracture stages of *Striped bass* scale, (b) fracture mechanism of bony and collagen layers, and (c) SEM images of fracture process from the bony and collagen sides [7].

them with the thermoplastic polymers (i.e., polycarbonates (PC)). The maximum load-carrying capability was observed in the head scale at the loading rate of 50 mm/s. This is because of the presence of high mineral content in the external layers of fish scales at the head region.

The natural dermal protection offered by fish scales is a unique combination of highly mineralised external "bony" and soft internal "collagen" layers. These hierarchical structures (anisotropic) enable several pathways to improve the existing dermal armors in a revolutionary manner [23]. Therefore, hardness analysis of fish scale (micro/nano-indentation) is an important aspect to determine the mechanism involved in designing bioinspired armors. Nano-indentation tests were performed on *P. senegalus* scale (see the four layers of scale in Fig. 4d and Fig. 18) [23] to measure the penetration resistance, elastic and plastic properties. The results of the tests (Fig. 18a) indicated that the indentation modulus (approximately from 62 GPa to 17 GPa) and hardness (approximately from about 4.5 GPa to 0.54 GPa) decrease with increasing indentation depth [56]. The mechanical properties are different for each layer, but the maximum indentation modulus of about 62 GPa and hardness of about 4.5 GPa are found for the bony layer (i.e., the external layer of the fish scale). With increasing depth, the collagenous dentin layer exhibits less mineral content than the ganoine layer, but more mineral content than the osseous basal plate [21]. The microstructure of the outer ganoine layer is "rod"-like pseudo-prismatic crystallites of apatite. Isopedine (the third layer) consists of orthogonal collagen layers similar to the plywood structure. The innermost layer has a collagen fiber-rich zone with a maximum thickness of 300 µm.

The detailed results for nano- and micro-indentation of different layers (i.e., ganoine to the bone plate, and epoxy) are shown in Fig. 19 [23]. The study reported that the outer ganoine layer is a multilayer structure which offers a stiff barrier against nano- to micro-indentation. The penetration load dissipates through the underlying dentin layers. The entire process of load dissipation is controlled by the anisotropic structure of the fish scale. This condition is the underlying design principle for developing new bioinspired materials. Each layer of the scale was scanned using tapping-mode atomic force microscopy (TMAFM) after the indentation tests, and the measurement confirmed the plastic deformation

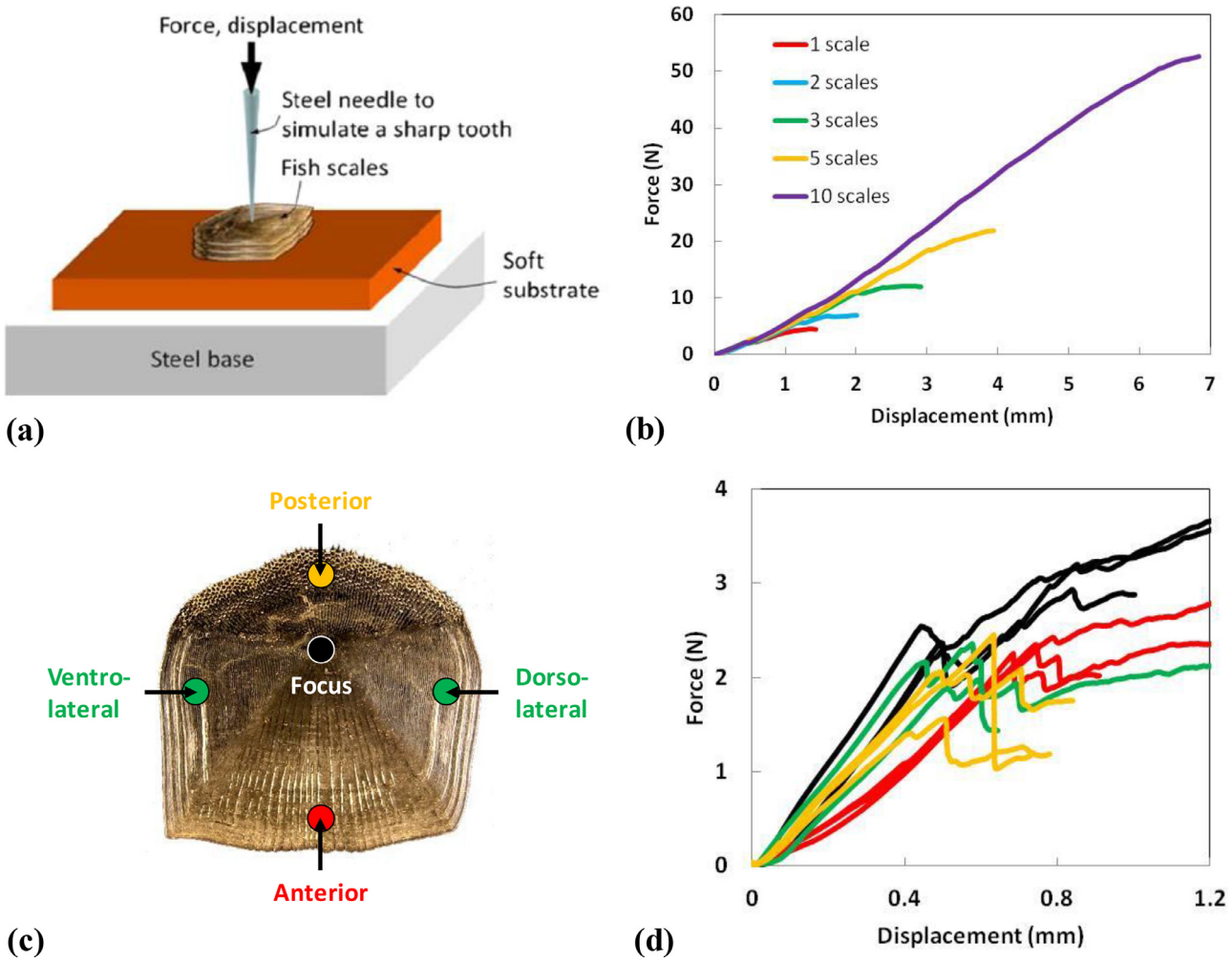

Fig. 16. (a) Puncture tests on Stacked fish scales, (b) force versus displacement curves for 1, 2, 3, 5, and 10 scales, (c) different positions (anterior, posterior, dorso-lateral, and ventro-lateral) in a fish scale, and (d) force versus displacement curves for different positions in a fish scale [55].

of the scale (see Fig. 19). For the micro-indentation at 1 N maximum load, the TMAFM and optical micrographs showed that the ganoine layer is under a brittle-failure condition and the fracture is a circumferential crack pattern.

The stress generated during the indentation can be compared with the finite element analysis (FEA) for the discrete and gradient structures of the scale. The results from the FEA show a good agreement with the measured results (Fig. 20) [23], and the simulation can be used for stress analysis of scale for predicting various failure modes. For example, no cracks were observed at 0.5 N load, the deformation followed an elastic-plastic pattern, and nearly half of the sample showed the circumferential cracking at 1 N load. All the samples showed circumferential cracks at a load of 2 N (Fig.s 20b-c). The cross-sectional SEM image (Fig. 20d) demonstrated the micro-cracking within the sublayers of isopedine layers. The generated cracks were in the orthogonal direction and arrested at the edges of the layers. The micrograph (Fig. 20e) of the ganoine-dentin junction indicated an important aspect of the junction, which contributes to the ability to arrest cracks.

The ganoine-dentin junction transfers the load to the underlying softer layers, and the stiff layer dissipates the load. A significant increase in the circumferential cracking (*S22>S11*) is beneficial as compared with radial failure. The isopedine layer prevents any catastrophic failure because the structure is in the form of plywood, which fails layer by layer. Therefore, the unique combination of various layers simultaneously provides different mechanical properties. The multilayer FEA showed the stress pattern generated during the indentation test (Fig. 21a-c). The simulation results can be useful in understanding various aspects, such as layer-by-layer stress pattern, stresses at junctions, and discrete and gradient models at 1 N indentation load.

Allison et al. [20] performed nano- and micro-indentation (Vickers) tests on *A. spatula* scales to analyse the damage and cracking patterns along with mechanical protective mechanisms. The tests were performed to characterise the mechanical properties such as elastic modulus and hardness (Fig. 22). The mechanical properties found from this test are similar to those obtained by Bruet et al. [23], as shown in Fig. 15a, i.e., the ganoine layer has the maximum hardness and elastic modulus. In another study, the micro-indentation was performed to examine the fracture behavior under the indentation test [20]. Fig. 23a-d show the micrographs for the indentation performed at loadings of 1, 5, and 10 N on the surface of scale specimens. The circumferential cracks (Fig. 23d) were visible under 5 and 10 N loads due to the shear stress generated by the indenter. The cracking in all layers of the scale can be observed in Fig. 24a. The cracks in the ganoine layer are brittle and

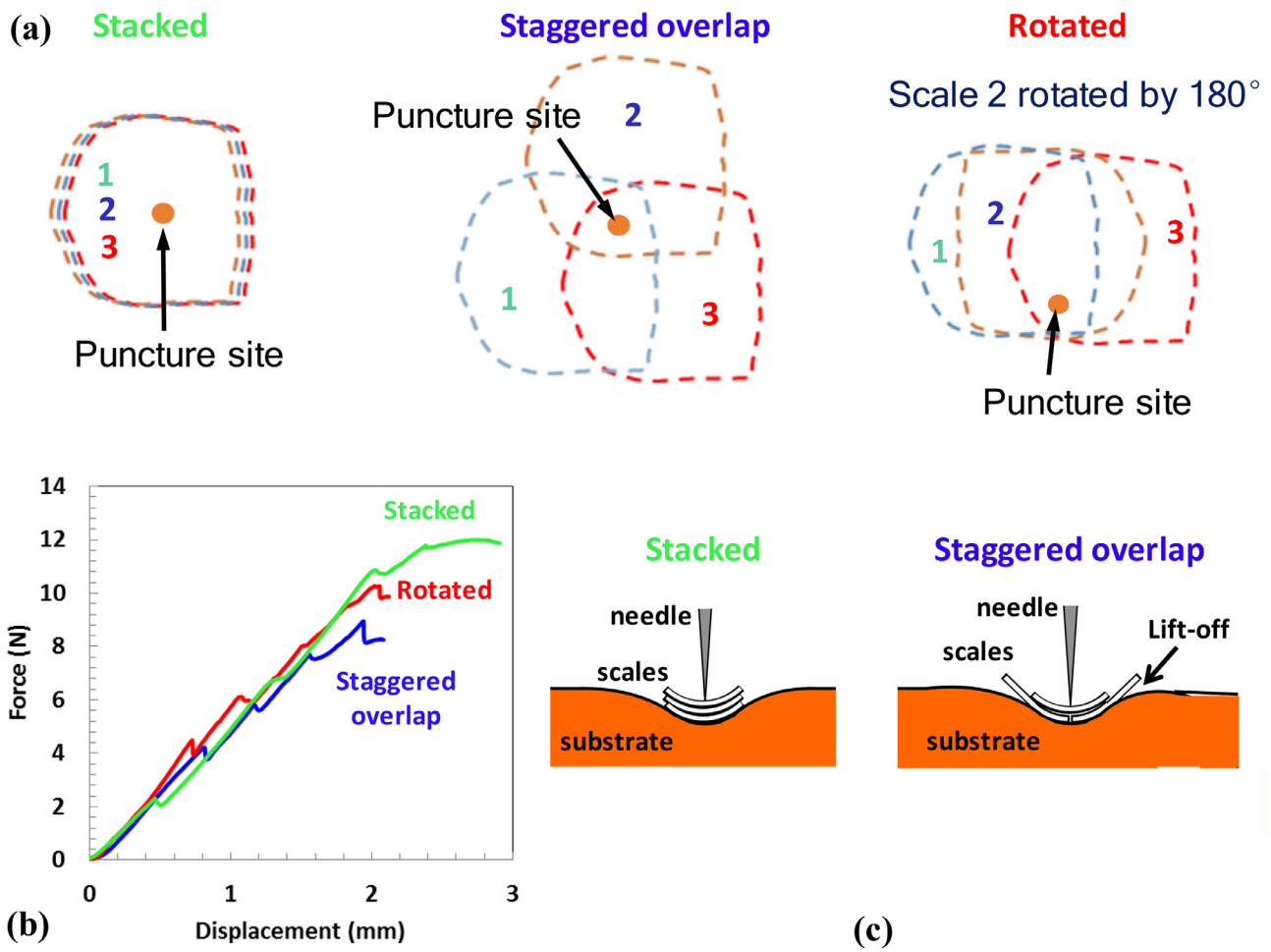

Fig. 17. (a) Puncture site for various arrangements (stacked, staggered overlap, and rotated), (b) force versus displacement curves of puncture test for different arrangements, and (c) deformation mechanisms of scales with different arrangements [55]

relatively smooth (Fig. 24b). Fig. 24c displays the delamination at the interface during micro-indentation. The growth of crack and fiber bridging in Fig. 24d shows a ductile failure of the inner layer. These cracks (developed in *A. spatula* [20] and *P. senegalus* scales [23]) are advantageous because deformation and fracture are located at the indentation point instead of propagating throughout the material.

3.3. Fracture properties of teleost fish scales

Fish scales have outstanding stiffness, but undesirable brittleness leads to a lack of toughness [59]. However, the unique combination of hard/stiff external layers with internal soft layers offers outstanding fracture toughness in fish scales. Yang et al. [60] studied the fracture toughness of alligator gar (*A. spatula*) fish scales. Three-point bending tests were performed to measure R-curves (crack-resistance curves) as a function of crack initiation and propagation, along with three different orientations under dry and wet conditions (see Fig. 25a-b). For orientation 3, the highest slope (in R-curves) was measured owing to the orientation of collagen fibers relative to the crack growth. For orientations 1 and 2, the tubule and collagen fibers were slightly angled with the crack propagation direction. Orientation 3 exhibited a nearly perpendicular orientation for the tubule and collagen fibers with respect to the crack growth direction, as shown in Fig. 26a-c. The 3D visualisation of crack propagation for dry and wet scales is provided in Fig. 26d-e, respectively, which confirmed that the crack in wet samples propagates relatively in a straight line (Fig. 26e). The SEM images of the crack path in Fig. 26f-g show similar propagations.

Both samples (dry and wet) were in good condition after the fracture toughness test [60]. The good condition is because cracks only appeared during the test, and there was no major fracture. For the dry scale samples, cracks propagated in the direction of tubules and collagen fibers. For the wet scale condition (physically realistic condition), the crack did not follow the direction of tubules and collagen fibers. The anisotropy and plasticity of wet samples can help in preventing any catastrophic failure in any situation. Dastjerdi et al. [61] proposed a new fracture test technique for the fracture toughness analysis of the whole scale (Fig. 27a), and the bony and collagen layers extracted from modern teleost fish. Small steel plates were clamped to the sample to transfer uniform loading and to provide controlled crack propagation during the tests. The bony layer (high mineralisation) was insensitive to the notch, which indicates the high toughness of the fish scale. The properties of the whole scale were significantly affected by the pre-crack positions over the scales, as shown in Fig. 27b-c. Additionally, the direction of crack propagation was also highly influenced by the fiber orientation in the sublayer [61].

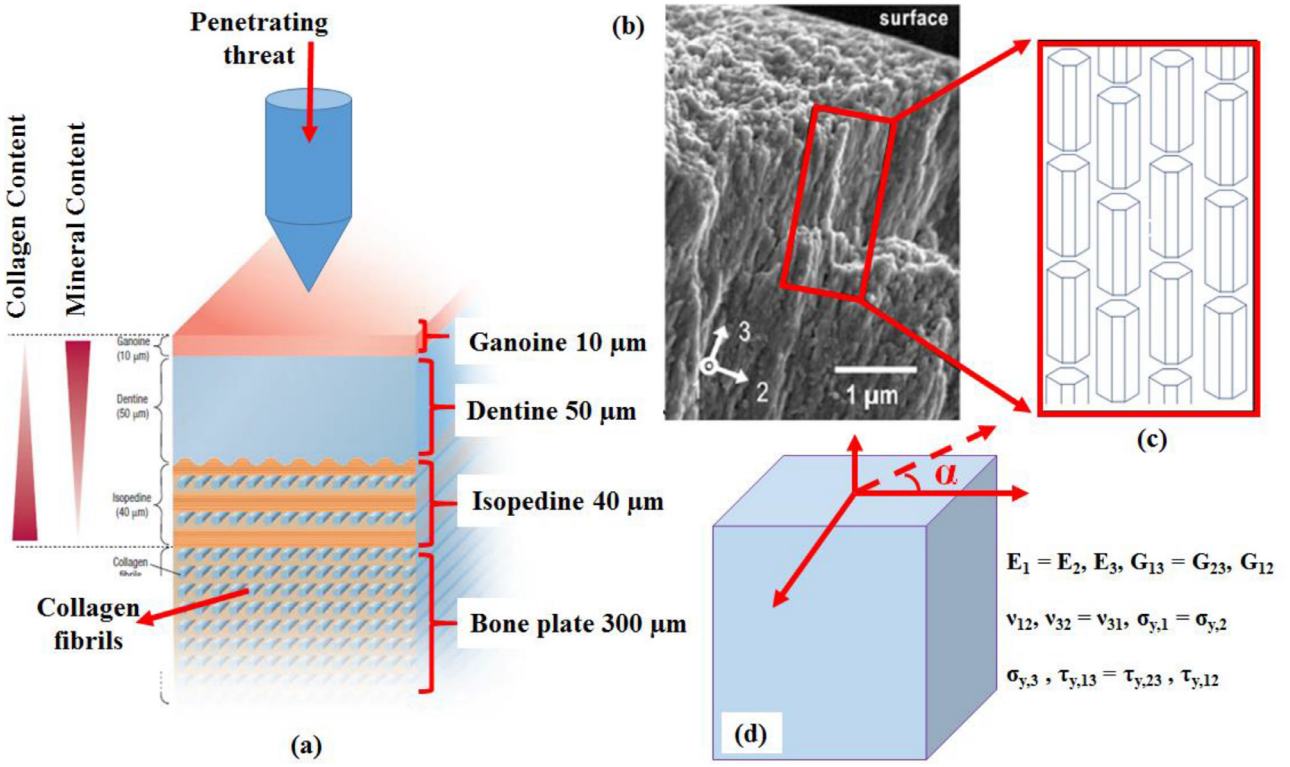

Fig. 18. (a) Four different layers of *Polypterus senegalus* scale [57], (b) anisotropic constitutive behavior of outermost individual layer (organic-inorganic nanocomposites), (c) anisotropic structure of ganoine layer, and (d) inherent crystalline anisotropy [58].

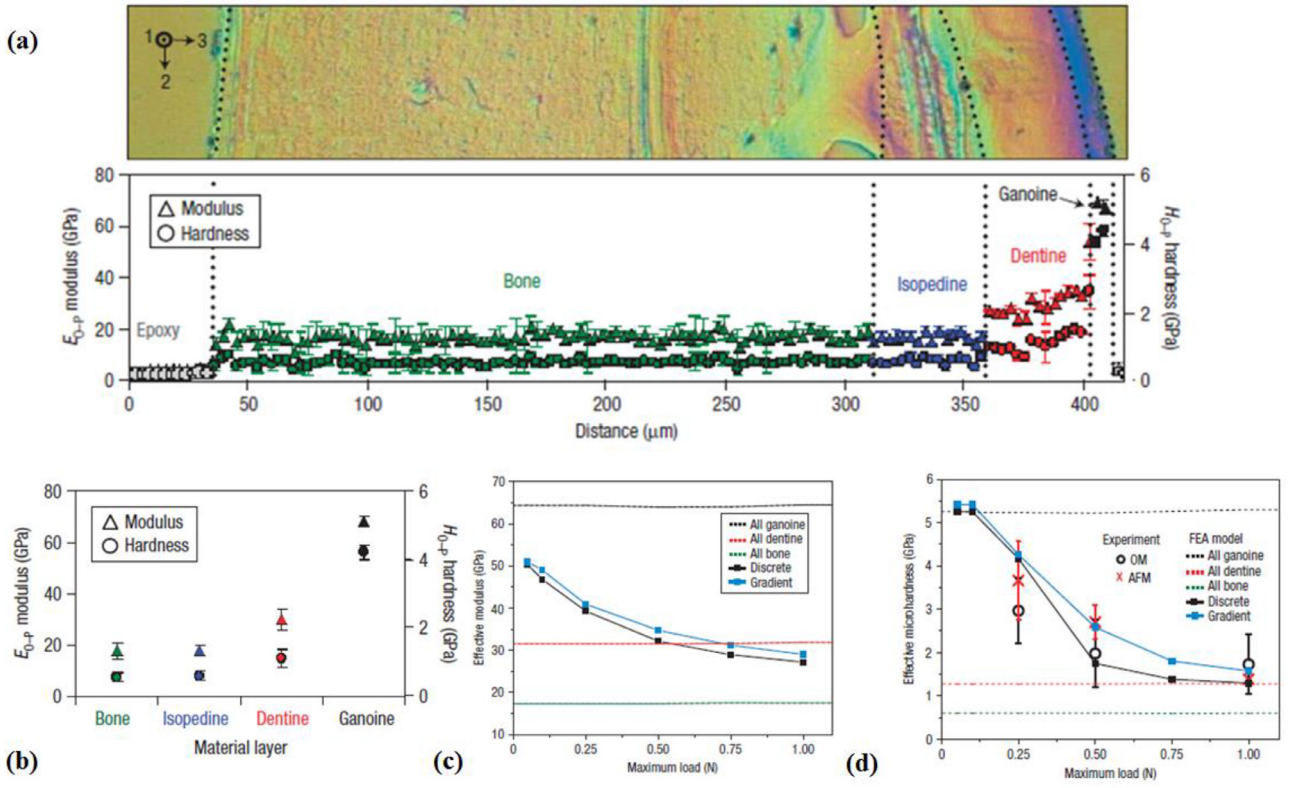

Fig. 19. (a) Indentation modulus and hardness as a function of distance across the scale thickness (epoxy layer represents the embedding zone), (b) nano-indentation values for modulus and hardness for different layers, (c) micro-indentation property, i.e., simulated effective indentation modulus, and (d) simulated effective micro-hardness and experimental value [23].

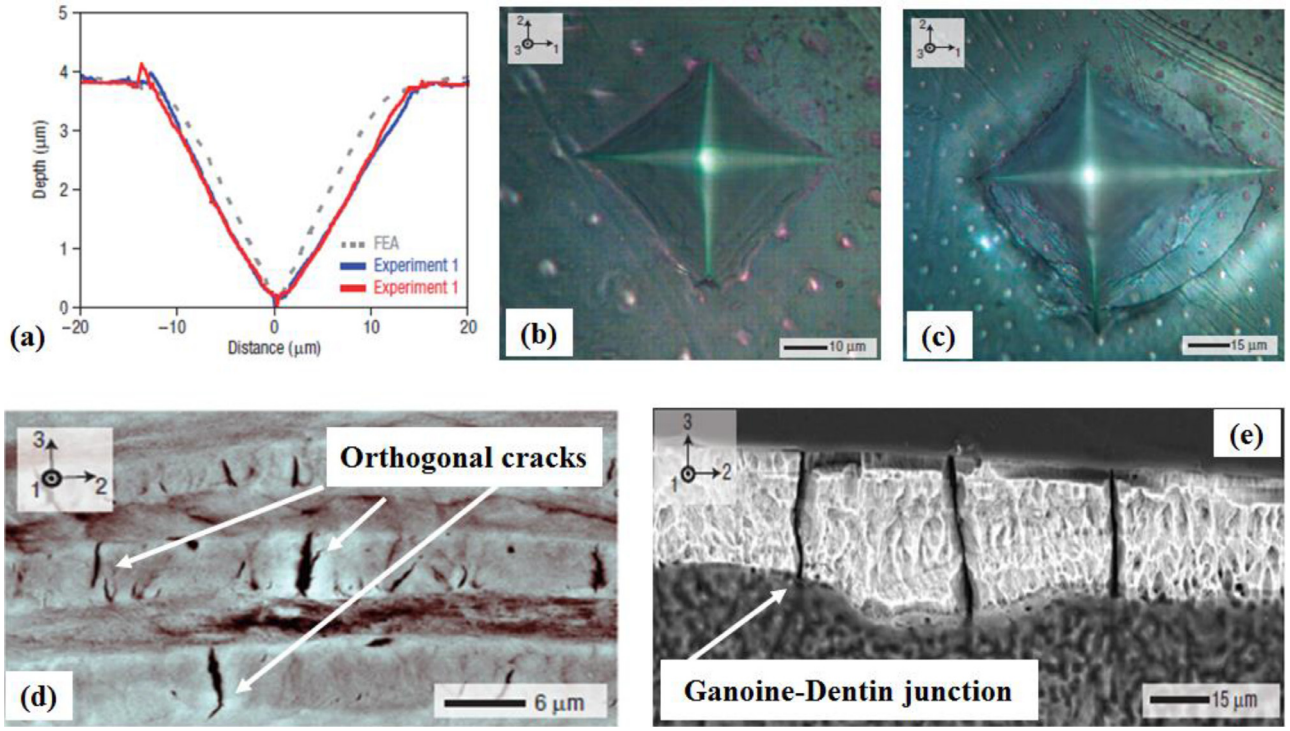

Fig. 20. (a) Experimental and FEA results for 1 N load nano-indentation, (b) indented surface at 1N load, (c) circumferential cracks in micro-indentation at 2 N load, (d) cross-sectional image of isopedine layers, and (e) sectional view of ganoine and dentine layers [23].

Structural and mechanical analyses of the fish scale are crucial to designing a bioinspired armor. The fracture testing results showed that the fracture toughness of fish scales was higher than that of bone (1–10 kJm^{-2}) [62] and mammalian skin (10–20 kJm^{-2}) [63]. The optical image (Fig. 28a) was also analysed to exhibit the defibrillated structure, thereby elucidating the mechanisms involved in fracture. The individual scales' interlaminar fracture toughness test with experimental results is shown in Fig. 28b-c [61]. Murcia et al. [64] investigated the effects of temperature variation (−150 °C–21 °C) on *C. carpio* scales. The scale samples were collected from three locations, i.e., head, middle, and tail (similar to Fig. 10). The testing samples were punched at three different orientations (0°, 45°, and 90° with the longitudinal axis), as shown in Fig. 11c. Tear tests (mode III) were further performed to calculate the fracture toughness of the fish scales at various temperatures. This investigation revealed that the scales from the head region (0° orientation with longitudinal axis) have the maximum fracture resistance and tear energy (see Fig. 29). The maximum resistance to fracture energy was measured at 50 ± 25 kJm^{-2} for the head scales with a 0° orientation (Fig. 29a-c). The fracture resistance decreases due to the continuous decrease in elasmodine layers (external and internal) from the head to the tail regions (Fig. 29d-f). A reduction in fracture toughness is observed with decreasing temperature (from ambient to liquid nitrogen temperature), and nearly 75% reduction in work fracture of scales is also observed. This result indicates the significance of considering temperature variations for the bio-inspired armor design due to their direct influences on the fracture (tear) performance, depending on the environmental conditions where the bio-inspired design will be used. The mechanical performance (tear resistance) also decreases with decreasing anisotropy (from head to tail).

Recent findings on the toughness of *Arapaima* scale by Yang et al. [65] proved that the two-layered *Arapaima* scale is one of the toughest flexible biological materials. This scale also has high load-bearing and substantial deformation resistance capabilities without showing any catastrophic failure. The collagen lamellae can resist deformation because of the reorientation, separation, delamination, shearing, and twisting of collagen fibers.

4. Bioinspired human body armor

The bio-inspired concepts have proven their importance in designing new structures that can eliminate (or minimise) the design constraints related to fundamental mechanical properties such as brittleness, toughness, and ductility. One of the prevalent examples is the removal of brittleness in glass and ceramics [66]. The manufacturing concept for building new structures inspired by natural phenomena is the layer-by-layer deposition similar to the brick-and-mortar pattern [67], additive manufacturing, rapid prototyping, and self-assembly [68–71]. This concept allows developing new strategies to combine materials with distinguished properties such as toughness and hardness with higher strength. For example, the nacre and conch shell structures combine hard and soft phases arranged in the brick-and-mortar pattern at the microscopic level [72]. As a result, the crack direction follows a particular pattern between the interfaces during the crack propagation in the nacre, resulting in a tortuous path [73]. This specific crack propagation behavior contributes to higher energy dissipation, making the nacre structure 'a best design' for high-performance bio-inspired material. For taking advantage of the nacre's structure, the ice-templating technique can be used to mix liquid-phase pre-

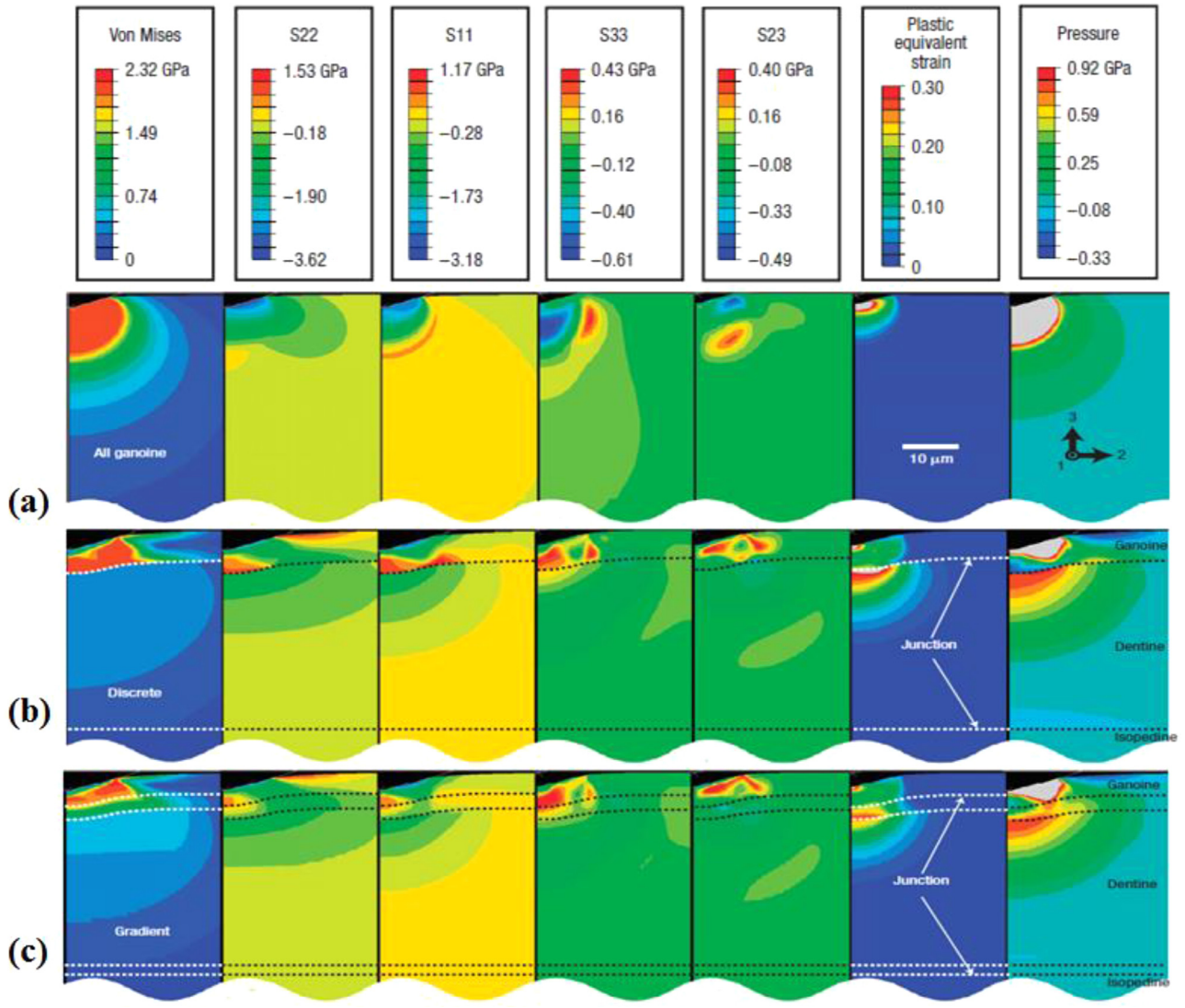

Fig. 21. Multilayered finite element simulation for stress contours, plastic strain, and pressure fields of a *P. senegalus* scale for three models: (a) all ganoine, (b) discrete, and (c) gradient models for 1-N-maximum-load indentation showing von Mises stress field, *S22* (normal stress on the plane perpendicular to the two axes), *S11* (normal stress on the plane perpendicular to the one axis), *S33* (normal stress on the plane perpendicular to the three axes), *S23* (shear stress on the plane perpendicular to the three axes acting in the two directions), plastic equivalent strain after fully unloading, and pressure at maximum depth when fully loaded [23].

cursors such as silica and calcium in the gaps produced in alumina nanoparticles during the sintering process [74]. Bouville et al. [74] used this concept to fabricate bulk ceramic designs without any ductile phase, offering high strength (470 MPa), toughness (22 MPa $m^{1/2}$), and stiffness (290 GPa). Other natural designs, such as fish scale, tooth enamel, stomatopod dactyl club, and bone structure, can also be made, combining various properties with a distinct geometric structure that provides superior mechanical properties. Therefore, the various design factors responsible for the unique mechanical properties in teleost scales are sought in this study.

Besides being an ancient creature, fishes are the most successful vertebrates. The main reason for this is their ability to improve themselves over the evolution period and adapt to a new environment. The fishes currently make up nearly 50% of the population of all living vertebrates [75,76]. Such a massive number of populations infer their ability to survive from the initiation of life on Earth. The *Lorica Plumata* and *Lorica Squamata* armors were inspired by fish scales [77], and they provided protection for the human body [40]. With the development of engineering technology, researchers have studied the compositions and structural patterns of fish scales (or skin), and the specific and unique features [78,79] that are responsible for their survival from predator attacks. Researchers have also used many advanced techniques such as 3D printing to develop advanced fish-scale-inspired flexible body armors for personal protection [80–83].

Meyers et al. [52] discussed the concept of flexible composites with minimum tensile strain at mineral layers. These layers display flexural resistance capability when the axis is parallel to the edges of the corrugations, as shown in Fig. 30a-b. Zimmermann et al. [84] focused on the "Bouligand"-type structure in natural dermal armors. They found that the "plywood"-type structure (i.e., "Bouligand"-type structure) of collagen fibers is the key factor for high toughness and ductility in *arapaima*'s scale. This scale shows tough behavior from the outer side because of its high mineral content. The inner layers with "Bouligand"-type structure provide the ductile response under the tensile test. The reorientation of a lamina takes place as a reaction to stress generation with the

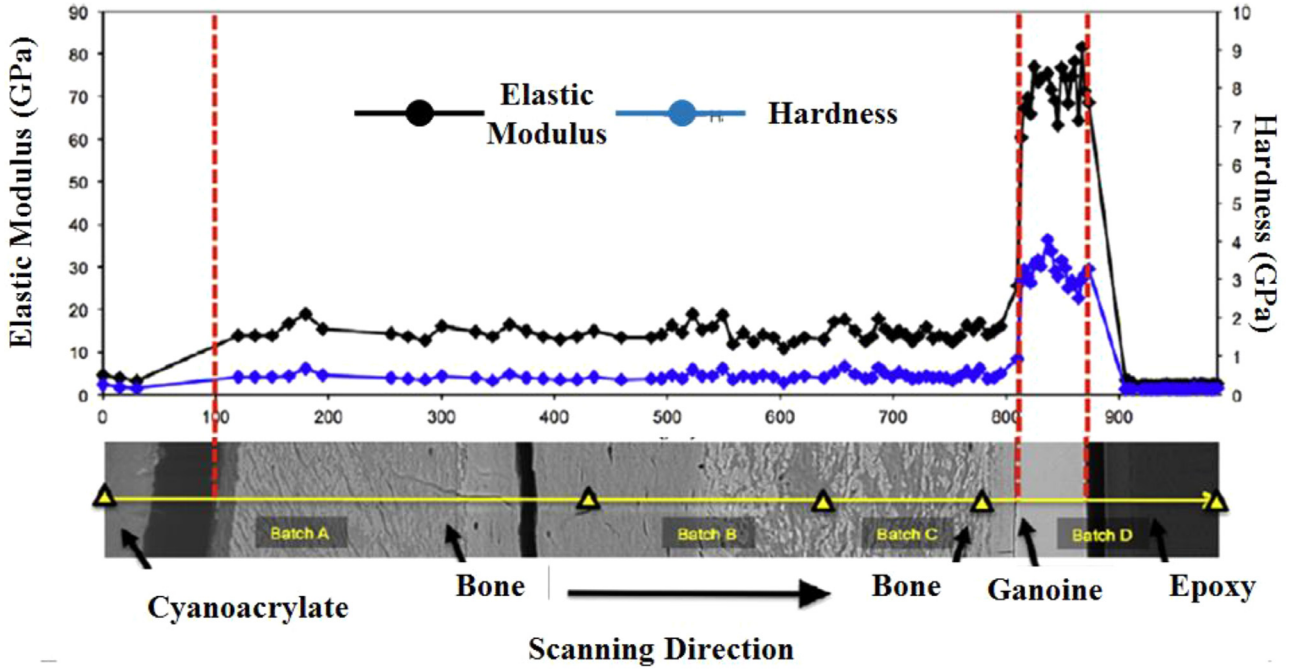

Fig. 22. Mechanical properties for the *A. spatula* scales determined from nano-indentation tests (total length of the cross-sectional scale is ~800 μm) [20].

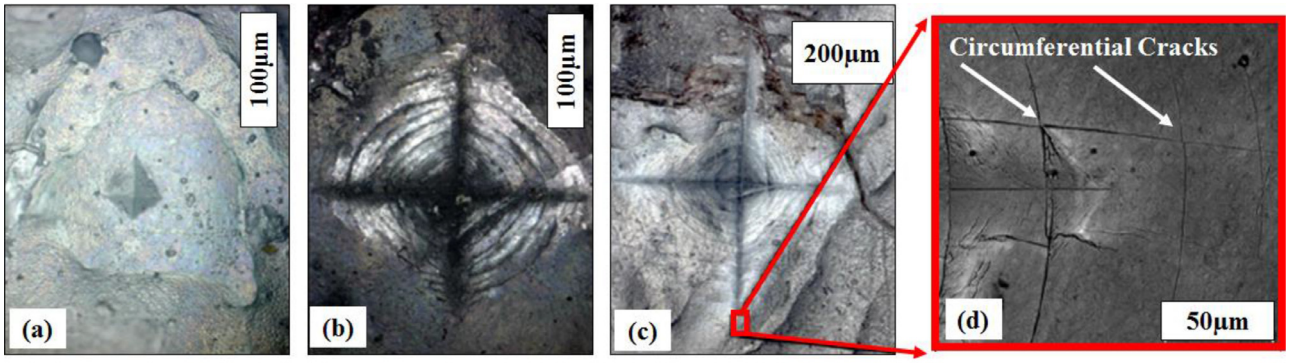

Fig. 23. Optical micrographs of Vickers micro-indentation tests at (a) 1 N, (b) 5 N, and (c) 10 N loadings on the surface of the *A. spatula* scales, and (d) SEM image of circumferential cracks developed at 10 N loading [20].

stress-induced in collagen layers (isotropic). The lamellae rotate in the direction of stress-induced in the tensile test, and fibrils slide or stretch along with the principal orientation (Fig. 30c-f). Hence, this ductile behavior prevents the breaking of the scale under tensile loading.

Martini et al. [85] studied the mechanical interactions (between hard scales and soft-substrate tissues) that help in load distribution due to the unique optimum arrangement of the scales on fish skin. The findings of this study are important for developing bioinspired designs. As shown in Fig. 31a, the vertically applied force on a single scale caused free movement of the substrate layer, and the reaction force was opposite to the direction of the applied force. In the presence of neighboring scales (Fig. 31b-c), the free movement of the substrate layer was hindered, and the direction of the reaction force changed toward the horizontal line. This feature is vital for a bioinspired design as the neighboring scales directly interfere with the reaction force. The slanted geometry (Fig. 31c) was stable and distributed the load uniformly. The orientation and geometry of hard and soft components helped in improving penetration resistance and offered high flexibility in movement. Fig. 31d shows the flexural compliance subjected to major and minor overlapping conditions with different types of scale arrangements and geometrical modifications. The puncture resistance versus flexural compliance (Ashby chart) characteristics for all considered design parameters can be seen in Fig. 31e.

Different parts of the body move with the movement of every individual, and hence the body requires greater flexibility. Rudykh et al. [86] presented a multifunctional and competitive design for protection and termed it as "protecto-flexibility," i.e., protection with flexibility. This design was fabricated using the 3D printing method. A range of microstructural arrangements was produced by varying the scales volume fractions of 0.1, 0.2, 0.3, and 0.4, and inclination angles of 10°, 20°, 30°, and 45° relative to the substrate. The proposed design (Fig. 32a-c) signified that the safety (provided by protective equipment) in terms of penetration resistance could be ensured without compromising the flexibility. The indentation

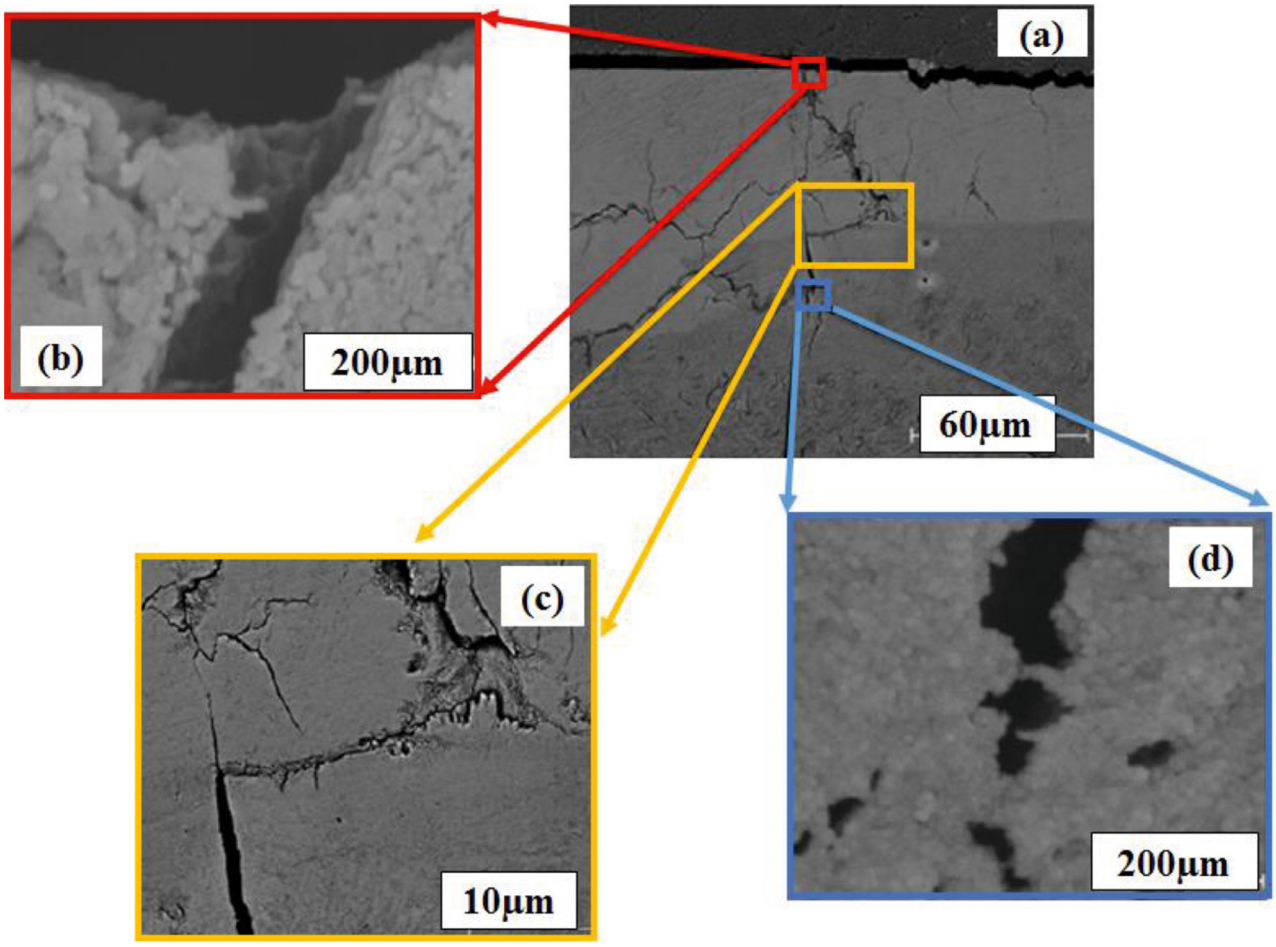

Fig. 24. (a) The tortuous path of the crack growing from ganoine layer to inner layers, (b) cracks in ganoine layers, (c) delamination at the interfaces, and (d) bridging at the crack tip in bony layers [20].

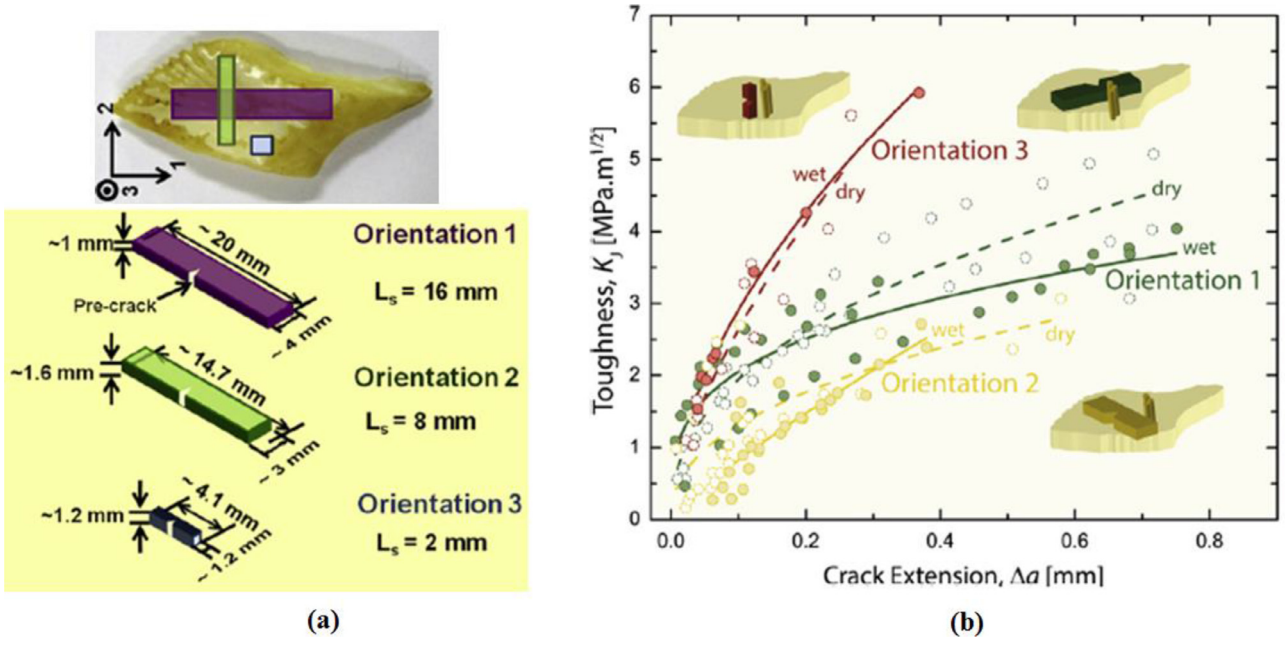

Fig. 25. (a) R-curve testing orientations with specimen dimensions, and (b) toughness versus crack extension for selected orientations under dry and wet conditions [60].

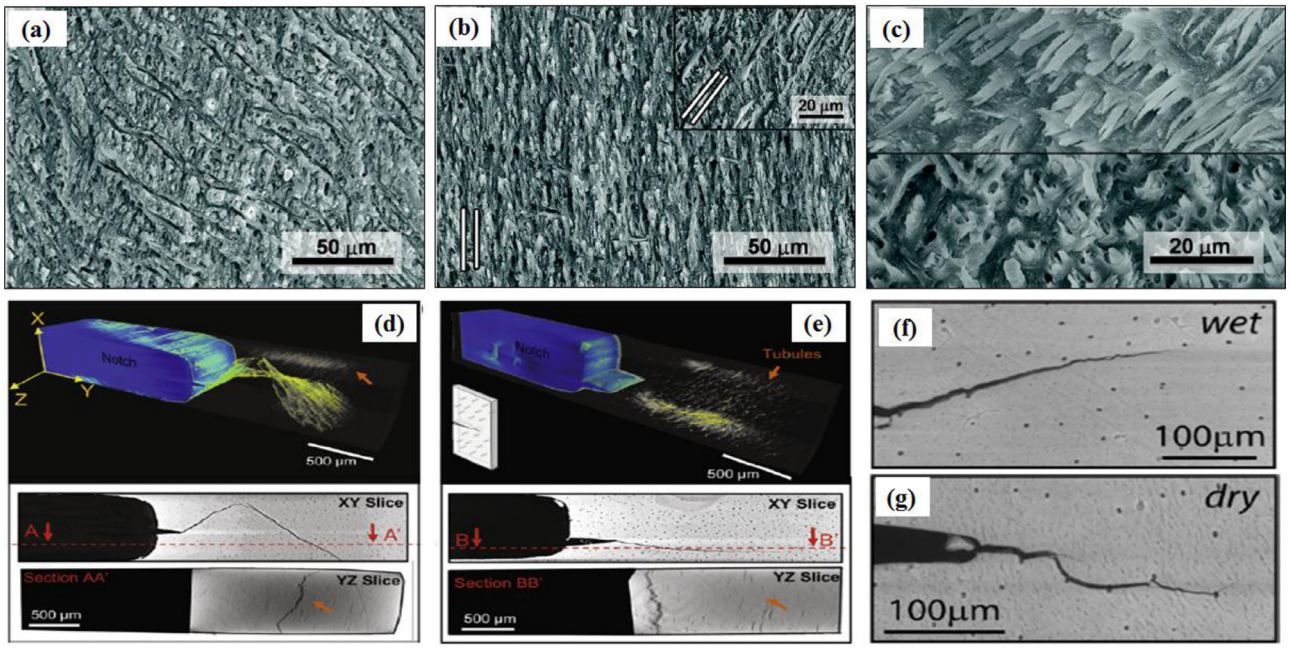

Fig. 26. SEM images of the fracture surfaces after crack growth in toughness tests and status of collagen fibers showing the crack growth after testing (a) orientation 1, (b) orientation 2, and (c) orientation 3 (see also Fig. 25a), representation of visualised crack path in (d) dry scale, (e) wet scale, and (f, g) SEM images of crack growth [60].

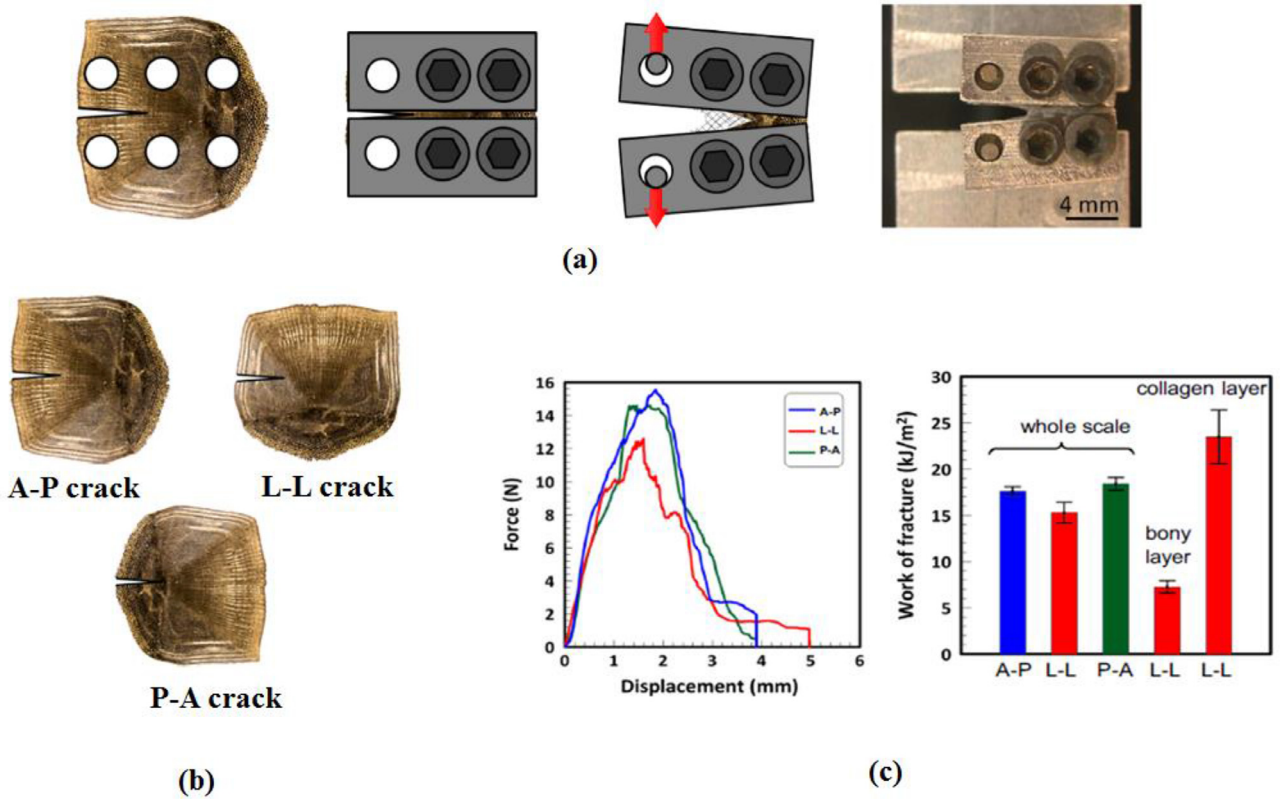

Fig. 27. (a) Miniature fixtures of stainless steel for fracture testing, (b) types of pre-cracks in preparing samples, (c) load-carrying capacity, and work of fracture with different samples [61].

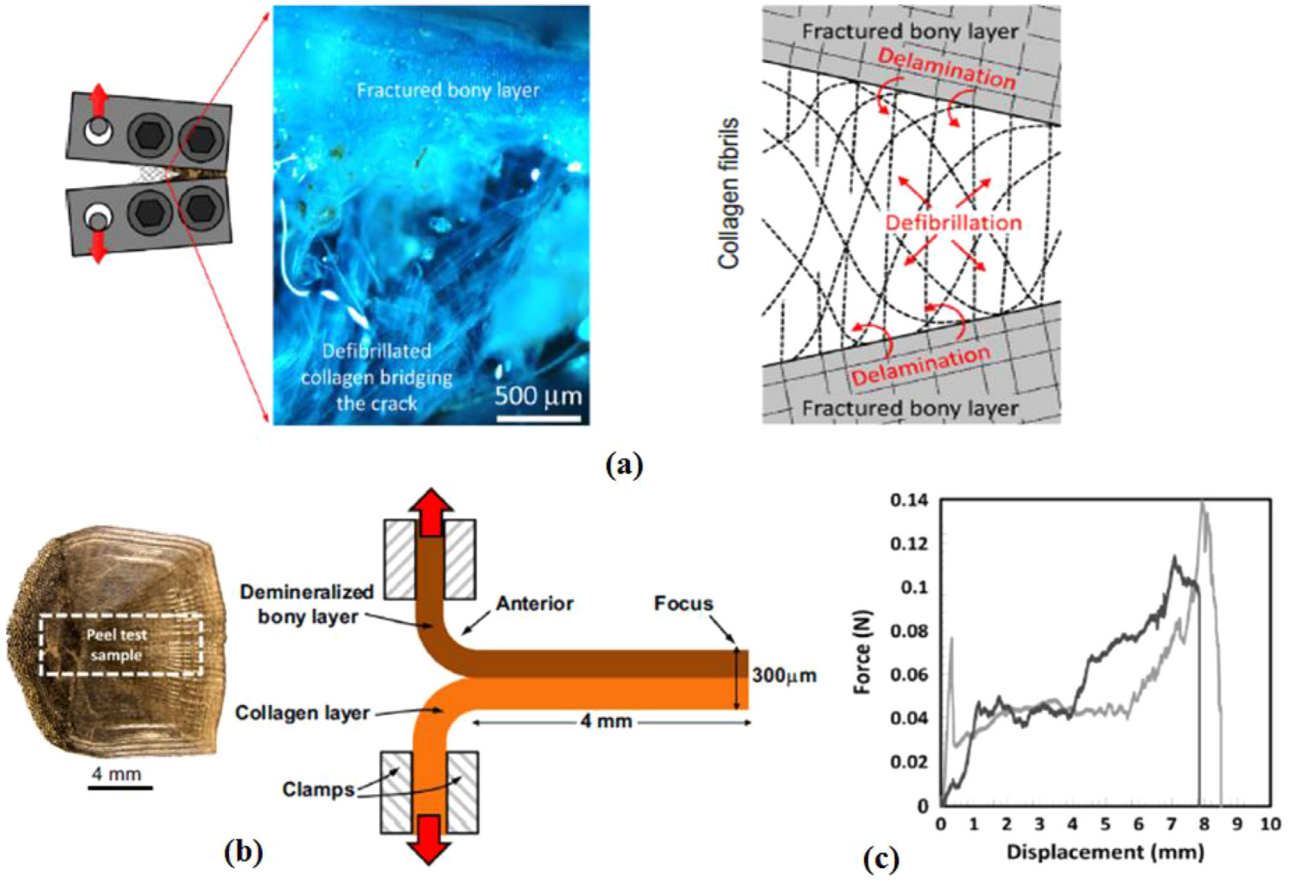

Fig. 28. (a) Optical image and schematic diagram of the softening region for fractured bony layer and defibrillated crack bridging of collagen fibers, (b) sample preparation and schematic diagram for peel test of a scale, and (c) force versus displacement curves obtained by peel test [61].

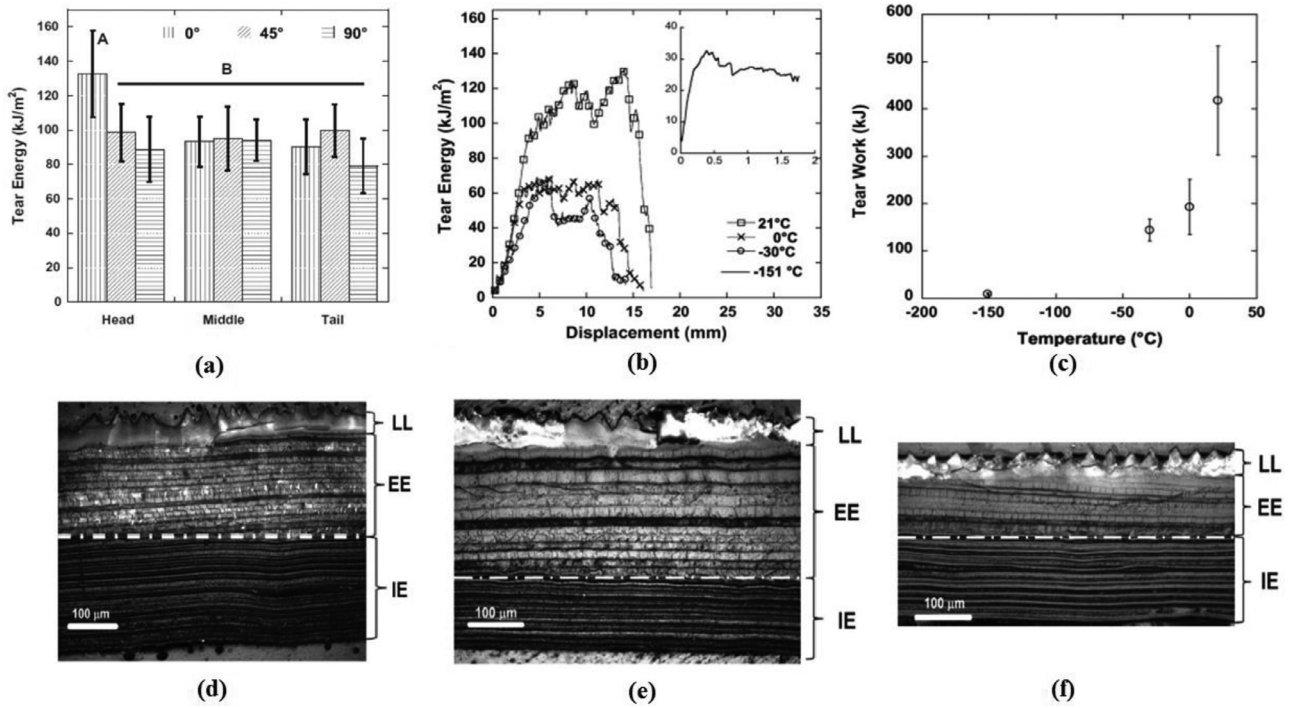

Fig. 29. (a) Tear energy responses for scales from the head, middle, and tail regions with 0°, 45°, and 90° orientations, (b) tear energy versus displacement, (c) tear work versus temperature; SEM images of the cross-sectional view of scales from the (d) head, (e) middle, and (f) tail regions for showing that the thickness is not equal in three regions [64].

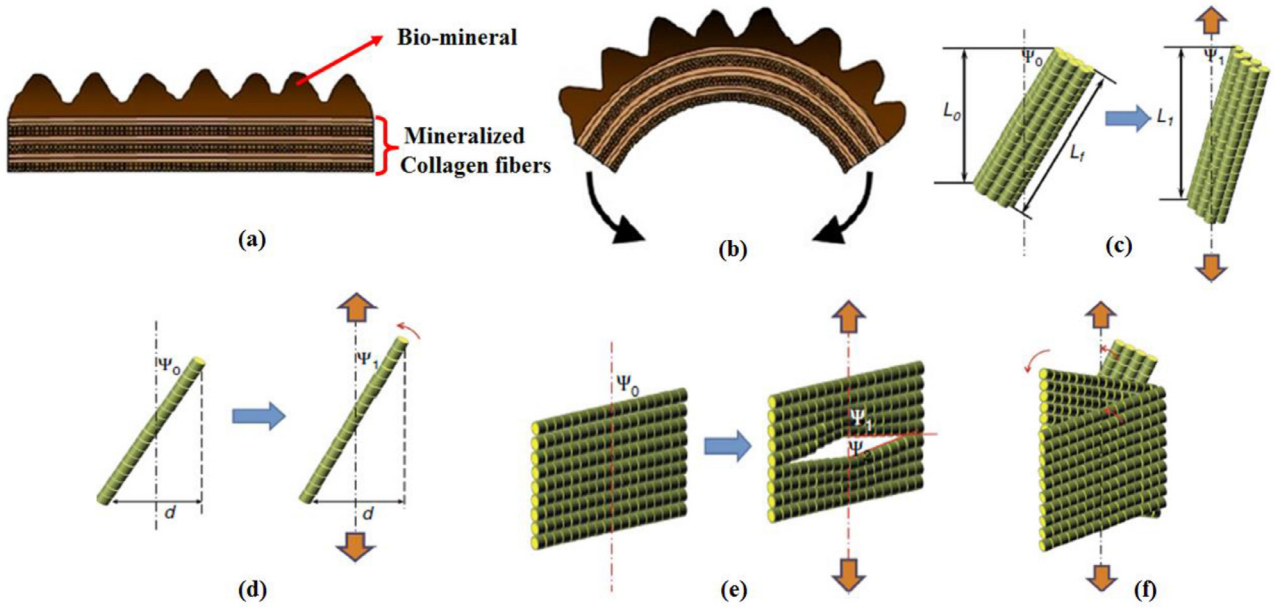

Fig. 30. Schematic diagrams of *'Arapaima's gigas* scale: (a, b) the channels in the mineralised layer for minimum tensile strain under loading in normal condition and flexed configurations [52], (c) rotation due to inter-fibrillary sliding in axis direction where $\psi 0$ reoriented to $\psi 1$ by changing length *L0* to *L1*, (d) stretching of collagen fibers, (e) tensile opening of the inter-fibrillary gaps, and (f) sympathetic lamella rotation [84].

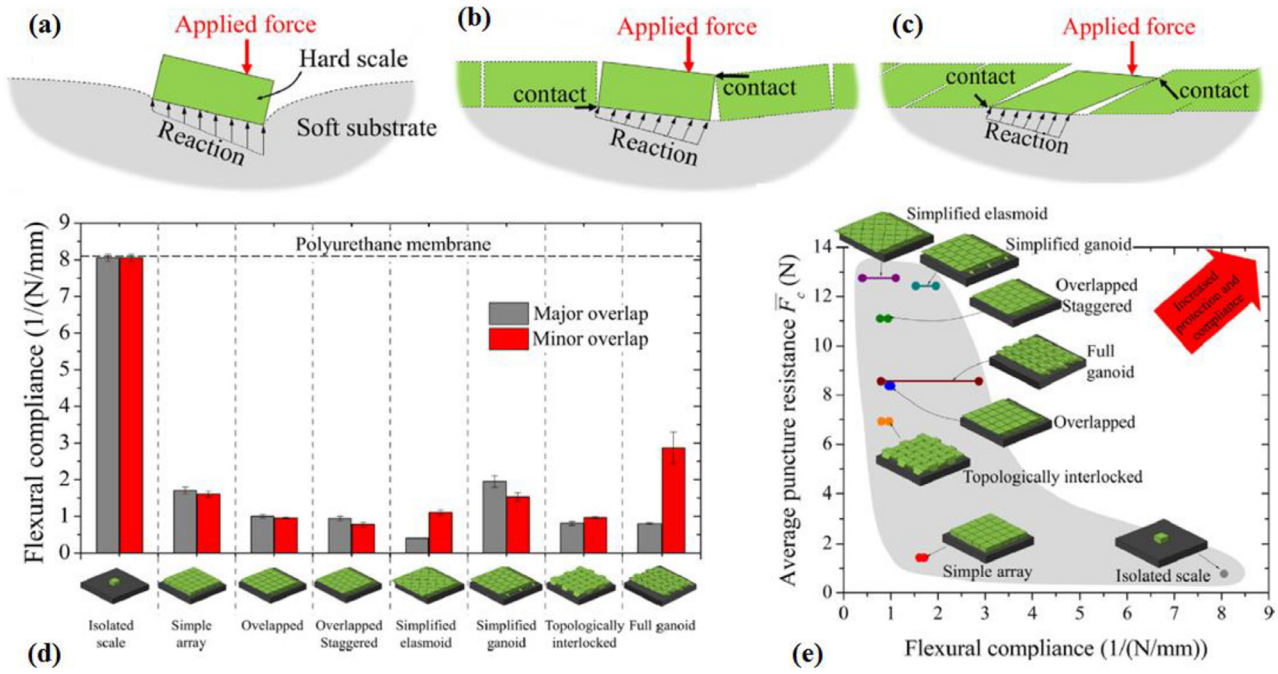

Fig. 31. Free body diagrams of scales resting over soft substrate under puncture tests: (a) single rectangular scale, (b) multiple scales surrounded by each other, (c) slanted scales which generate better interactions with neighboring scales, (d) comparison of the flexural compliance at small deflections for all proposed designs, and (e) the representation of flexural compliance and puncture resistance for the proposed designs [85].

force improves with the stiff volume phase of the protective design. The stiffest response is reported for the bi-layered scale with a volume fraction of 1.0, and the indentation force drops with an increase in the inclination angle.

The flexibility of the protective equipment depends on the compliant matrix shearing deformation mechanism. Therefore, careful selection of parameters (at the microscopic scale) can have the ability to attain multifunctional designs. Funk et al. [87] fabricated a bioinspired fish skin (in deformed and undeformed forms) using the combination of engineering materials (see Fig. 32d-e) for high flexibility with the improved mechanical performance [87]. This study found an essential key feature, namely, the flexural compliance required for unhindered motion. Synchronising the feature of the hard-mineralised layer with soft and flexible inner collagen

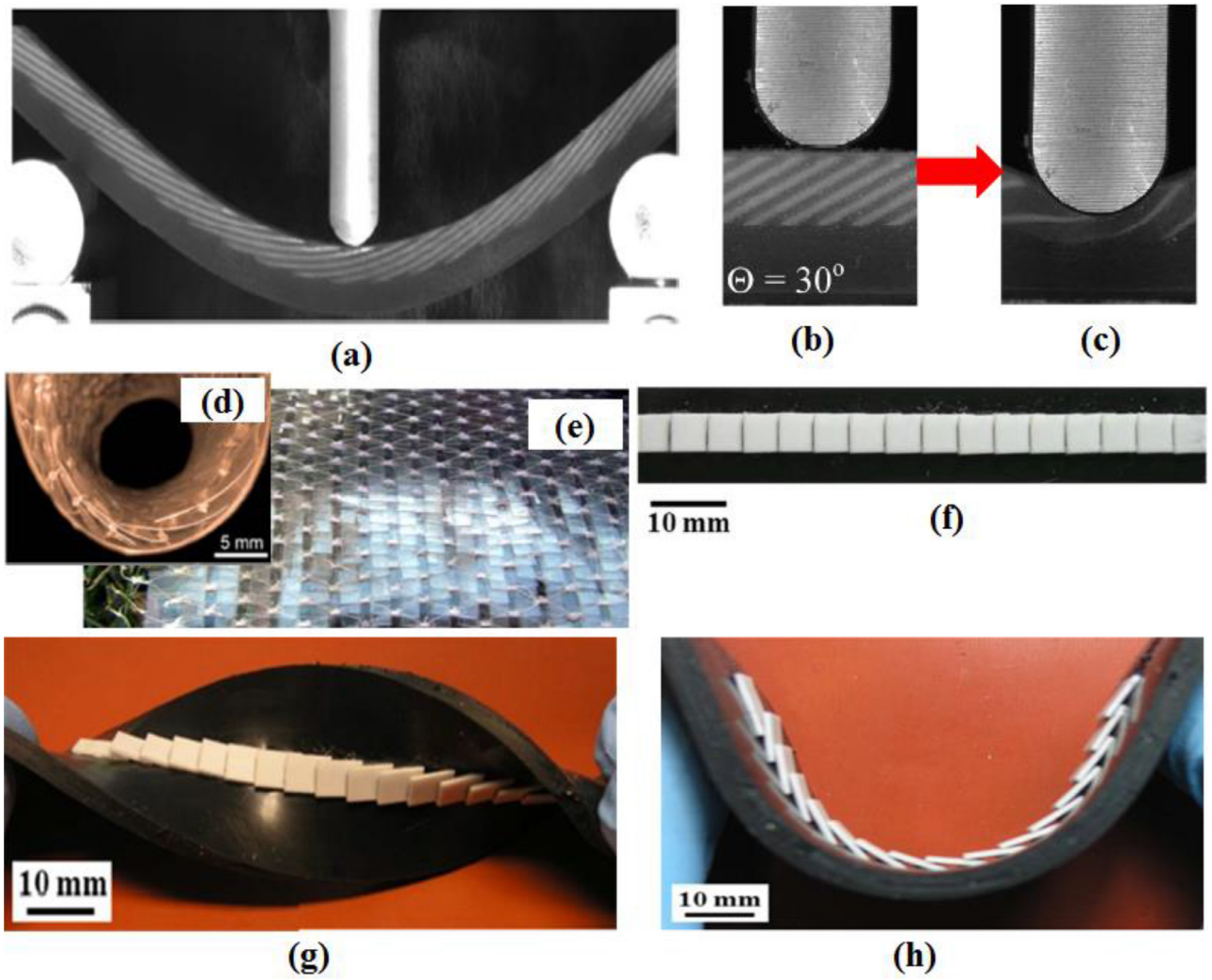

Fig. 32. Bio-inspired armor designs: (a-c) Micro-structured elasmoid scale armor [86] with angular scales for optimising the angle of scale for improved mechanical properties, (d, e) synthetic fish skin [87] with protective scales in rolled and flat view, respectively, (f) flexible membrane with ceramic scales for protection with flexibility [88], (g) torsional deformations, and (h) large flexural deformations.

layers is the most important challenge to achieve. Therefore, the human-made skin inspired by the teleost fish skin was modeled for in-plane and flexural deformations puncture tests. The outcome of this synthetic fish skin was similar to the performance of natural teleost fish. So, such skin can be used to protect the coating of soft materials because it is lightweight, transparent, and protective. The investigation of the stretch-and-release mechanism [88] of overlapped ceramic scales indicated that a bio-inspired design with a combination of hard ceramic scales and softer substrate ensures the possibility of large deformation under soft skin stretching conditions (see Fig. 32f-h).

The investigation by Funk et al. [87] highlighted that high-volume fractions of scales with the low angle of inclination offer the highest penetration resistance (penetration stiffness) (Fig. 33a-b), which increases with increasing depth. The penetration resistance enhances up to 40 times (without any perforation and fracture in the tested specimen), whereas the flexibility decreases five times. The maximum penetration resistance can be obtained using small-scale skin with large overlaps. The results of sharp puncture tests are shown in Fig. 33c-d, which present a comparison of scale skin with large overlaps, small overlaps, continuous aluminum (Al) strips, and silicon membrane. The highest penetration force was achieved from the scaled skin with large overlaps, but instantaneous failure was seen in this case. The small-overlap scaled skin showed multiple fractures during the test.

The four-point bending tests (Fig. 33e) for flexural performance showed the interaction of scales with intrados and extrados sides under loading. Scales on the intrados side performed well and achieved higher bending moment (with smaller scales and overlaps) as compared to the scales on the extrados side. On the opposite side, no scales interacted with one another, and they were, therefore, unsuitable for a bioinspired design. Synthetic skin can be applied as a suitable material for developing bioinspired designs. A bioinspired glove was designed (partially) with all the necessary parameters in terms of flexibility and strength, as shown in Fig. 34(a-f).

Another critical feature is the interfacing of two adjacent components of fish skin. The interfaces of natural designs of species (fishes) are in perfect geometrical shape with optimised fitting arrangements. These natural interfaces have remarkable mechanical features, i.e., the bonding parameters significantly influence the mechanical properties. Lin et al. [89] performed mechanical testing on 3D printed polymer prototypes with four types of interfaces (triangular, rectangular, trapezoidal, and anti-trapezoidal).

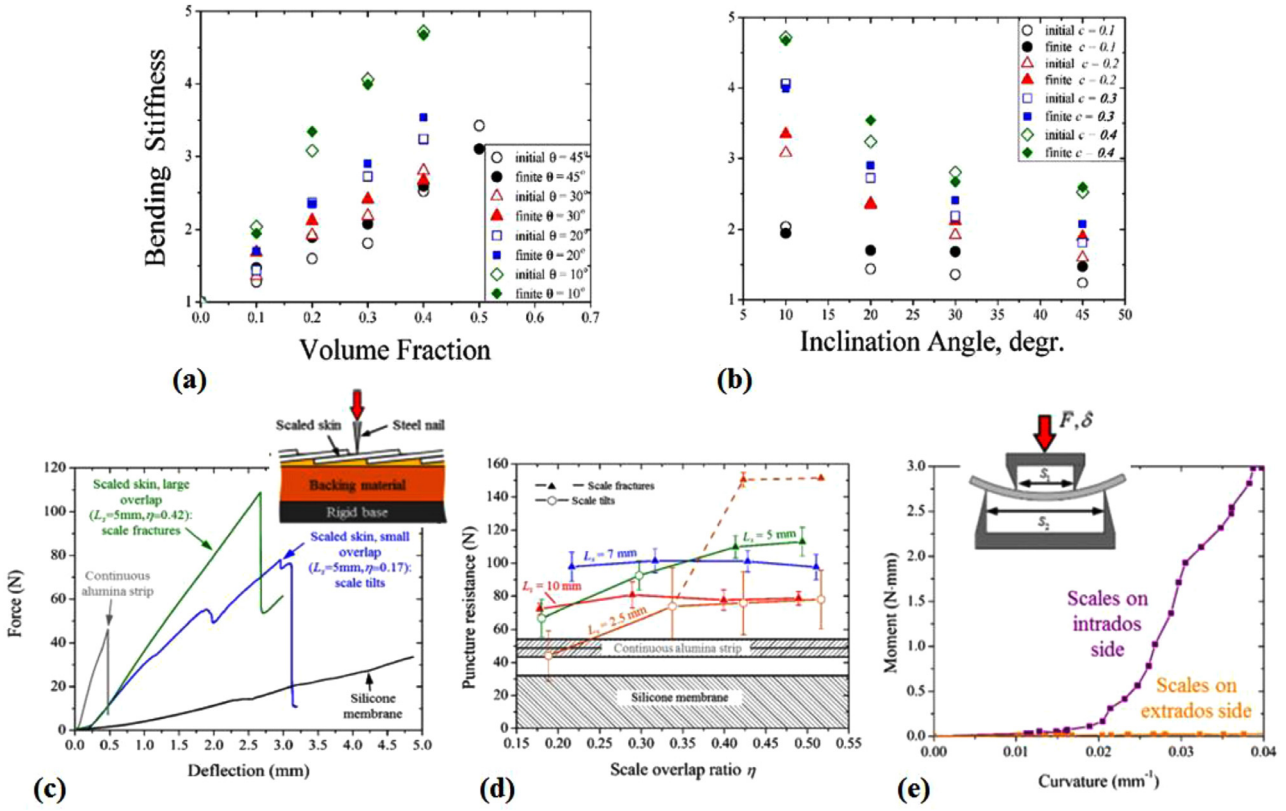

Fig. 33. (a, b) The effect of volume fraction and inclination angle of scales, respectively on the composite flexibility as a function of bending stiffness [86], (c) a comparison of force versus deflection curves for puncture test of synthetic skin, continuous alumina strip, and a silicone membrane, (d) puncture resistance versus scale overlap ratio (for different scale lengths), and (e) flexural response of the scaled skin (intrados and extrados sides) [88].

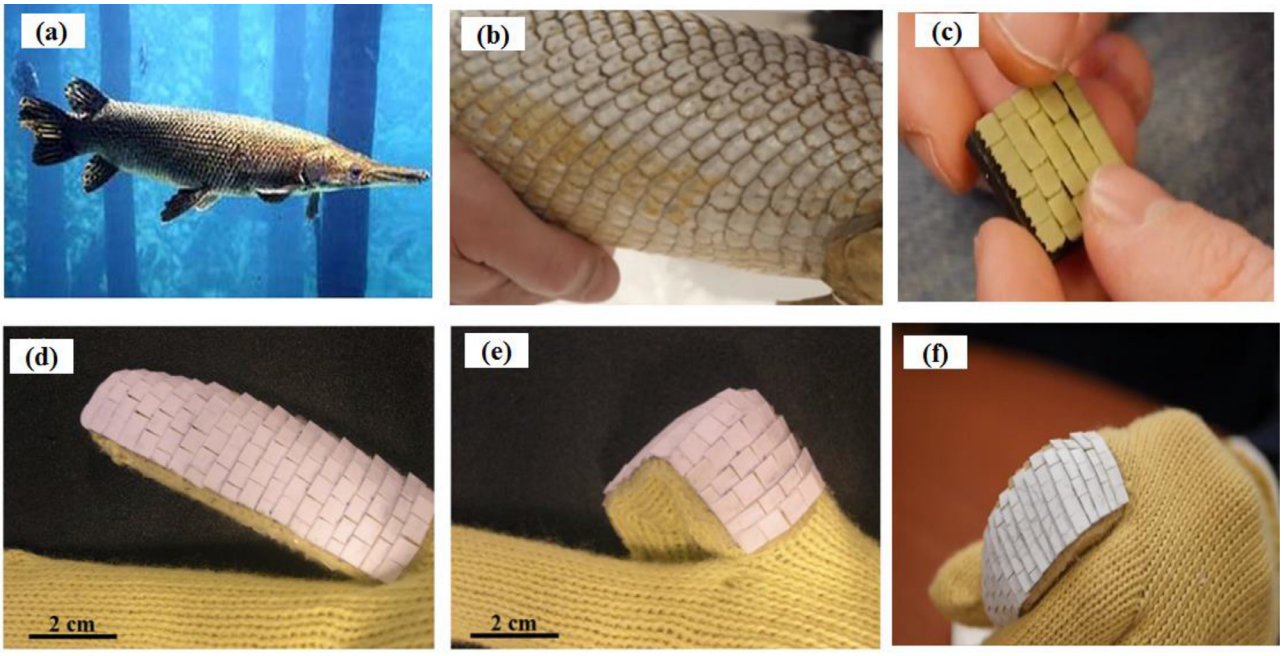

Fig. 34. (a, b) The garfish and the close view of scales, respectively, (c) development of hard ceramic plate and soft substrate-based armor structure inspired by garfish scale, (d-f) different positions for justification of flexibility in Kevlar glove (partially covered with synthetic scaled skin) [40].

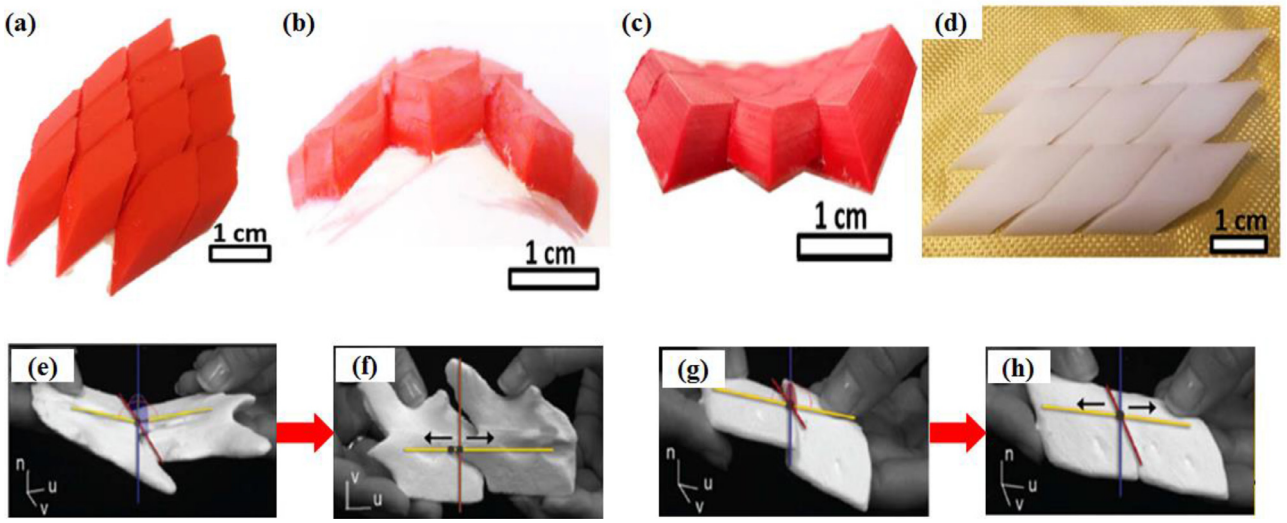

Fig. 35. (a-c) The gar scales produced by 3D printing using ABS (acrylonitrile, butadiene, and styrene) materials, (d) the assembled scale model (zirconia tiles) placed over Kevlar fabric for better flexibility [40]; (e, f) 3D-printed bichir fish and *Polypterus senegalus* head scales, respectively, and (g, h) tail scales and their interfaces, respectively, with higher flexibility, where (e, g) rotation around u-axis, (f, h) translation along u-axis [91].

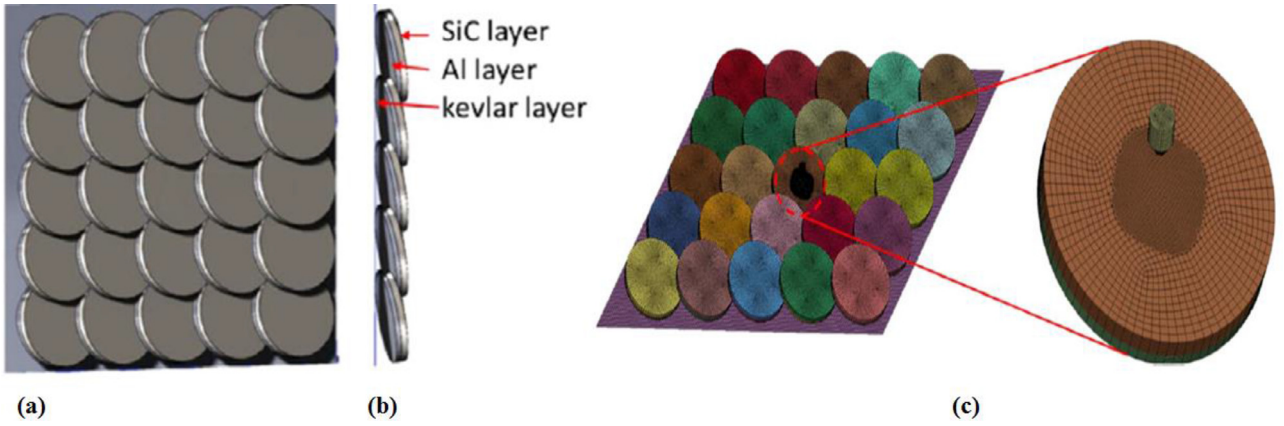

Fig. 36. (a) Fish scale inspired body armor vest design with overlapping scales, (b) cross-section of the vest with constituents, and (c) 3D FEA model for simulating ballistic performance using LS DYNA [92].

They found that mechanical properties such as strength, stiffness, and toughness depend on the interfacing parameters (i.e., bonding length, angle, and geometry). Each interfacing parameter affects mechanical properties. The angular arrangement of the tooth tip influences the overall performance (strength, stiffness, and toughness) of the fabricated structure.

The stress pattern and failure in the interfacial layer under tensile loading are affected by interfacial length. The triangular structure interfaces perform best because of uniform strain distribution. The most advanced manufacturing technologies (e.g., ABS for 3D printing and zirconia for machining) [40] can be used to manufacture (Fig. 35) replicate designs of fish scales (gar scales) with perfect shapes and fittings for interacting with one another. Nonetheless, these designs require a full-body biomechanism [76,90], which is relatively complicated.

Computational analysis using ANSYS/MATLAB/LS-DYNA can be performed for analysing a proposed model with various design parameters. These design parameters can be optimised using simulation tools well before the development begins, and they also save time and capital investment in manufacturing bioinspired designs. Liu et al. [92] optimised the thickness ratio of SiC/Al layers under high-velocity bullet impact conditions using LS-DYNA (Fig. 36a-c). The optimum overlapping ratio of 0.40 was determined from the simulations. Recently [93] it has been proved that the existing armor design parameters can be optimised for enhanced ballistic performance. Duro-Royo et al. [91] proposed a method of metamesh (Fig. 37) for fabricating a biomimetic armored surface for humans. The main advantage of this method is that it can fit with the host surface, i.e., flexibility in accordance with different body movements. This method addresses a few major research gaps in multiple functions of scales in terms of flexibility and to provide the best protective structures inspired by natural designs (e.g., *P. senegalus* fish).

Computational techniques can also simulate the performance of proposed designs under real-life situations. These designs can be fabricated for further testing under proper battlefield environments. In a recent study [91], the problem related to full-body biomechanics is solved to a certain extent using computational analysis. The final products can, therefore, be developed with unique interfacial interactions and good flexibility, as shown

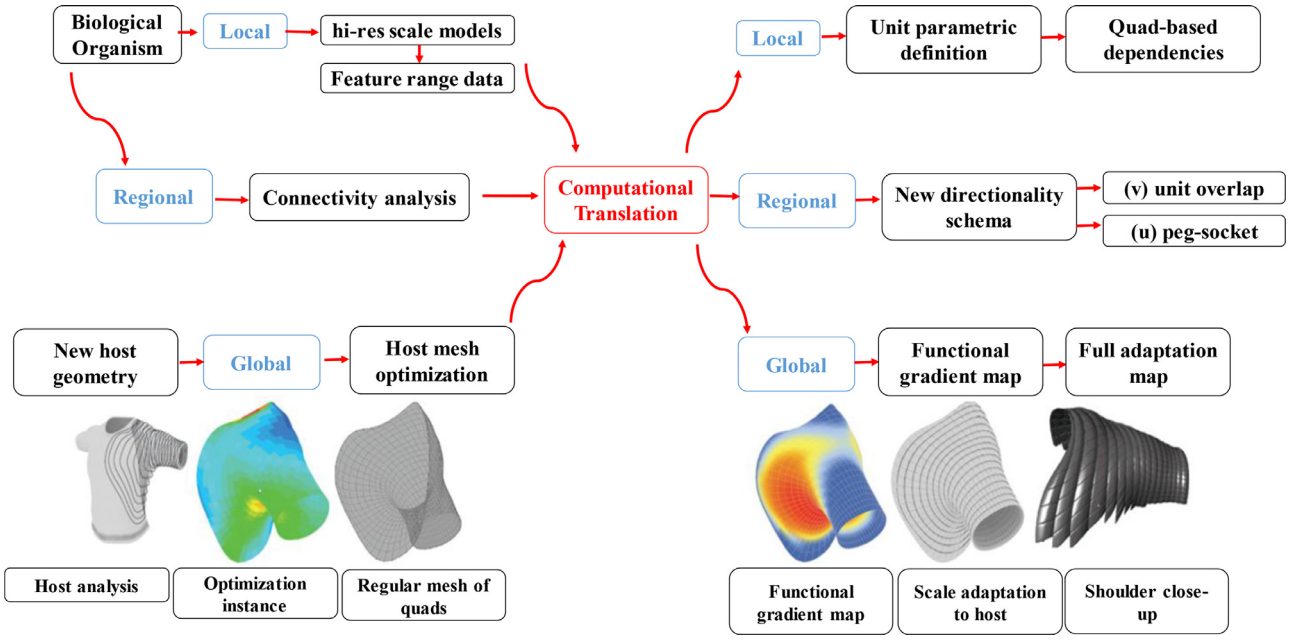

Fig. 37. A metamesh hierarchical computational model for designing human armor inspired by fish scales [91].

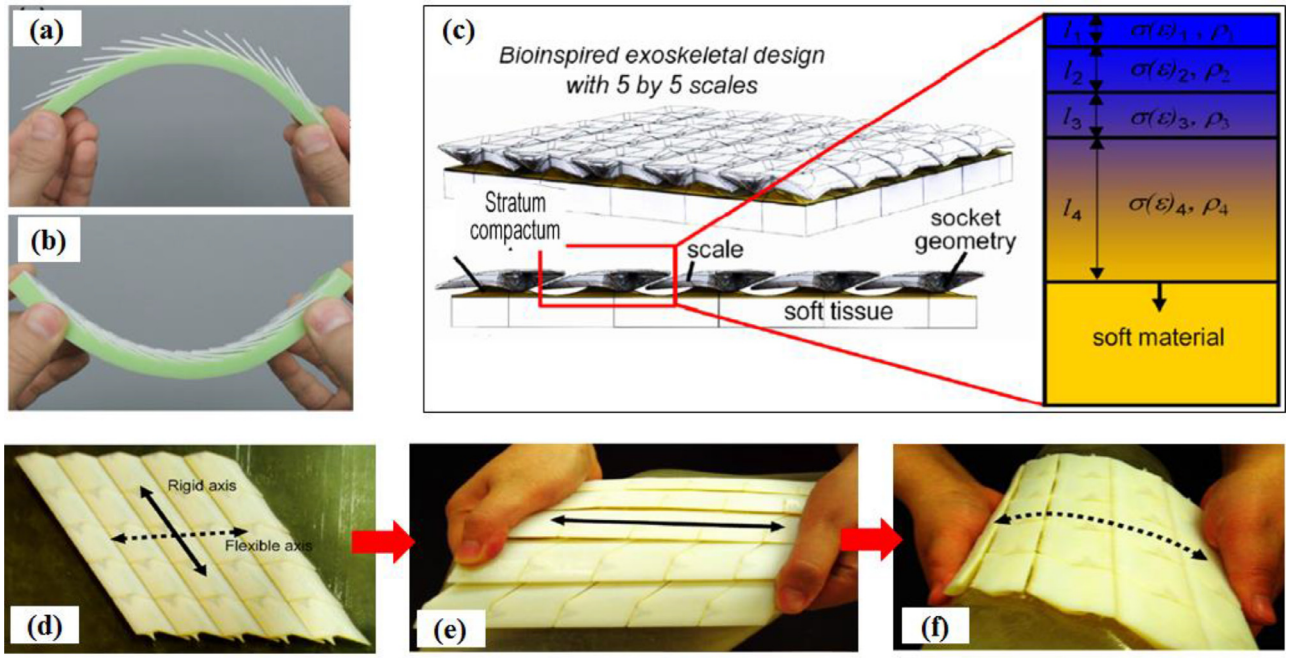

Fig. 38. (a, b) Manual demonstrations of 3D printed (thermo polymer) component under two opposite bending conditions [94], (c) concept of hybrid exoskeletal designs for 3D printing as a whole structure (based on *P. senegalus* scales) with the combination of hard and soft materials and varying thickness [81], and (d-f) 3D printed prototypes for anisotropic biomechanical behavior and flexibility under bending conditions [81].

in Fig. 38a-f. These designs can have an outstanding capability to resist penetrating loads and offer good flexibility. Although producing such kinds of armor components is at its initial stage, this opens up a new avenue for bio-inspired armor research and practical applications.

5. Conclusions

The teleost fish scale structure has outstanding mechanical properties that make it ideal for developing a new class of bio-inspired protective armors. The teleost fish scales are two-layered structure with varying mineral contents and designs at the microscopic level. The higher fracture toughness and hardness of the outer ganoine layer result from high mineral content in the "rod"-like structure. The inner layers are arranged in a plywood pattern or Bouligand structure. In each layer, the collagen fibrils are parallel to each other, and all layers have angular variations in the range of 45°–90°. The inner layer shows ductile behavior compared to the outer layer. Two-layered fish scale structure behaves like a laminated composite with high fracture toughness and offers multiple deformation mechanisms (e.g., fiber stretching, separation, reorientation, delamination, twisting, shearing, and fracturing) when

subjected to penetration. These attributes can provide outstanding penetration resistance with higher flexibility to the bio-inspired armors. However, combining two or more materials with different properties is the major challenge in creating a bio-inspired armor with higher toughness and flexibility.

The variations in mechanical properties of fish scales are caused by the dry and wet conditions, the anatomical positions, the anisotropy that decreases from the head to tail regions, the scale angles with overlapping areas, and the temperature change. Therefore, if one needs to develop a full-body bioinspired armor, all components (of the proposed design) must work together in a desired and optimal manner. With the available resources and manufacturing technologies, researchers can design body armors that are lightweight, flexible, and adequately strong. Notably, the advancement of full-body armors for human protection is still in the developing stage. Several research gaps related to achieving thin apparel-like flexibility, covering full-body parts (including shoulders, arms, and neck), and ease of repairing (replacement of damaged components) are yet to be investigated.

Declaration of Competing Interest

The authors declare no conflict of interest. They do not have any commercial or associative interest that represents a conflict of interest in connection with the work submitted.

Acknowledgements

This work was supported by the National Defense Science & Technology Innovation District Program (Grant Nos. 19-H863-03-ZT-003-033-01, 17-H863-03-ZT-003-008-06), High-level Talent Gathering Project of Hunan Province (Grant No. 2018RS3057), High-Tech Industry Science and Technology Innovation Leading Plan of Hunan Province (Grant No. 2020GK2079), and Science and Technology Program of Changsha City (kq1907115).

References

[1] P.-Y. Chen, A. Lin, Y.-S. Lin, Y. Seki, A. Stokes, J. Peyras, E. Olevsky, M.A. Meyers, J. McKittrick, Structure and mechanical properties of selected biological materials, J. Mech. Behav. Biomed. Mater. 1 (3) (2008) 208–226.
[2] W. Yang, I.H. Chen, B. Gludovatz, E.A. Zimmermann, R.O. Ritchie, M.A. Meyers, Natural flexible dermal armor, Adv. Mater. 25 (1) (2013) 31–48.
[3] Q. Chen, N.M. Pugno, Bio-mimetic mechanisms of natural hierarchical materials: a review, J. Mech. Behav. Biomed. Mater. 19 (2013) 3–33.
[4] L. Grunenfelder, N. Suksangpanya, C. Salinas, G. Milliron, N. Yaraghi, S. Herrera, K. Evans-Lutterodt, S. Nutt, P. Zavattieri, D. Kisailus, Bio-inspired impact-resistant composites, Acta Biomater. 10 (9) (2014) 3997–4008.
[5] D.H. Evans, The Physiology of Fishes, CRC Press, 1993.
[6] E.S. Goodrich, in: On the Scales of Fish, Living and Extinct, and Their Importance in Classification, Zoological Society of London, Wiley Online Library, 1907, pp. 751–773.
[7] D. Zhu, C.F. Ortega, R. Motamedi, L. Szewciw, F. Vernerey, F. Barthelat, Structure and mechanical performance of a “modern” fish scale, Adv. Eng Mat. 14 (4) (2012) B185–B194.
[8] J. Bereiter-Hahn, L. Zylberberg, Regeneration of teleost fish scale, Comp. Biochem. Physiol. A Physiol. 105 (4) (1993) 625–641.
[9] H. Onozato, N. Watabe, Studies on fish scale formation and resorption, Cell Tissue Res. 201 (3) (1979) 409–422.
[10] H. Quan, W. Yang, E. Schaible, R.O. Ritchie, M.A. Meyers, Novel defense mechanisms in the armor of the scales of the “living fossil” coelacanth fish, Adv. Funct. Mater. 28 (46) (2018) 1804237.
[11] I.H. Chen, J.H. Kiang, V. Correa, M.I. Lopez, P.-Y. Chen, J. McKittrick, M.A. Meyers, Armadillo armor: mechanical testing and micro-structural evaluation, J. Mech. Behav. Biomed. Mater. 4 (5) (2011) 713–722.
[12] F. Barthelat, Biomimetics for next generation materials, Philos. Trans. R. Soc. Lond. A 365 (1861) (2007) 2907–2919.
[13] T. Ikoma, H. Kobayashi, J. Tanaka, D. Walsh, S. Mann, Microstructure, mechanical, and biomimetic properties of fish scales from Pagrus major, J. Struct. Biol. 142 (3) (2003) 327–333.
[14] J.W. Hawkes, The structure of fish skin, Cell Tissue Res. 149 (2) (1974) 147–158.
[15] F. Neave, Origin of the teleost scale-pattern and the development of the teleost scale, Nature 137 (3477) (1936) 1034–1035.
[16] L. Zylberberg, G. Nicolas, Ultrastructure of scales in a teleost (Carassius auratus L.) after use of rapid freeze-fixation and freeze-substitution, Cell Tissue Res. 223 (2) (1982) 349–367.
[17] D. Zhu, C. Zhang, P. Liu, L.A. Jawad, Comparison of the morphology, structures and mechanical properties of teleost fish scales collected from New Zealand, J. Bionic Eng. 16 (2) (2019) 328–336.
[18] U.G. Wegst, H. Bai, E. Saiz, A.P. Tomsia, R.O. Ritchie, Bioinspired structural materials, Nat. Mat. 14 (1) (2015) 23.
[19] O.P. Olson, N. Watabe, Studies on formation and resorption of fish scales, Cell Tissue Res. 211 (2) (1980) 303–316.
[20] P.G. Allison, M. Chandler, R. Rodriguez, B. Williams, R. Moser, C. Weiss Jr., A. Poda, B. Lafferty, A. Kennedy, J. Seiter, Mechanical properties and structure of the biological multilayered material system, Atractosteus spatula scales, Acta Biomater. 9 (2) (2013) 5289–5296.
[21] J. Daget, M. Gayet, F.J. Meunier, J.Y. Sire, Major discoveries on the dermal skeleton of fossil and recent polypteriforms: a review, Fish & Fish. 2 (2) (2001) 113–124.
[22] P.-Y. Chen, J. Schirer, A. Simpson, R. Nay, Y.-S. Lin, W. Yang, M.I. Lopez, J. Li, E.A. Olevsky, M.A. Meyers, Predation versus protection: fish teeth and scales evaluated by nanoindentation, J. Mater. Res. 27 (1) (2012) 100–112.
[23] B.J. Bruet, J. Song, M.C. Boyce, C. Ortiz, Materials design principles of ancient fish armour, Nat. Mat. 7 (9) (2008) 748.
[24] Y. Bouligand, Twisted fibrous arrangements in biological materials and cholesteric mesophases, Tissue Cell 4 (2) (1972) 189–217.
[25] F.J. Meunie, Spatial organization and mineralization of the basal plate of elasmoid scales in osteichthyans, Am. Zool. 24 (4) (1984) 953–964.
[26] F.J. Meunier, ‘Twisted plywood’structure and mineralization in the scales of a primitive living fish Amia calva, Tissue Cell 13 (1) (1981) 165–171.
[27] Z. Fang, Y. Wang, Q. Feng, A. Kienzle, W.E. Müller, Hierarchical structure and cytocompatibility of fish scales from Carassius auratus, Mater. Sci. Eng. C 43 (2014) 145–152.
[28] F.J. Vernerey, F. Barthelat, On the mechanics of fishscale structures, Int. J. Solids Struct. 47 (17) (2010) 2268–2275.
[29] M.R. Hebrank, J.H. Hebrank, The mechanics of fish skin: lack of an" external tendon" role in two teleosts, Biol. Bull. 171 (1) (1986) 236–247.
[30] M.R. Hebrank, Mechanical properties and locomotor functions of eel skin, Biol. Bull. 158 (1) (1980) 58–68.
[31] W. Yang, V.R. Sherman, B. Gludovatz, M. Mackey, E.A. Zimmermann, E.H. Chang, E. Schaible, Z. Qin, M.J. Buehler, R.O. Ritchie, Protective role of Arapaima gigas fish scales: structure and mechanical behavior, Acta Biomater. 10 (8) (2014) 3599–3614.
[32] P.-Y. Chen, J. McKittrick, M.A. Meyers, Biological materials: functional adaptations and bioinspired designs, Prog. Mater. Sci. 57 (8) (2012) 1492–1704.
[33] Z. Liu, M.A. Meyers, Z. Zhang, R.O. Ritchie, Functional gradients and heterogeneities in biological materials: Design principles, functions, and bioinspired applications, Prog. Mater. Sci. 88 (2017) 467–498.
[34] M.A. Meyers, J. McKittrick, P.-Y. Chen, Structural biological materials: critical mechanics-materials connections, Science 339 (6121) (2013) 773–779.
[35] M.J. Chon, M. Daly, B. Wang, X. Xiao, A. Zaheri, M.A. Meyers, H.D. Espinosa, Lamellae spatial distribution modulates fracture behavior and toughness of African pangolin scales, J. Mech. Behav. Biomed. Mater. 76 (2017) 30–37.
[36] J.W. Dunlop, P. Fratzl, Biological composites, Annu. Rev. Mater. Res. 40 (2010) 1–24.
[37] P. Fratzl, F.G. Barth, Biomaterial systems for mechanosensing and actuation, Nature 462 (7272) (2009) 442–448.
[38] F. Barthelat, Z. Yin, M.J. Buehler, Structure and mechanics of interfaces in biological materials, Nat. Rev. Mater. 1 (4) (2016) 16007.
[39] P. Fratzl, R. Weinkamer, Nature’s hierarchical materials, Prog. Mater. Sci. 52 (8) (2007) 1263–1334.
[40] V.R. Sherman, H. Quan, W. Yang, R.O. Ritchie, M.A. Meyers, A comparative study of piscine defense: the scales of *Arapaima gigas, Latimeria chalumnae* and *Atractosteus spatula*, J. Mech. Behav. Biomed. Mater. 73 (2017) 1–16.
[41] R.O. Ritchie, The conflicts between strength and toughness, Nat. Mater. 10 (11) (2011) 817–822.
[42] E. Arzt, Biological and artificial attachment devices: lessons for materials scientists from flies and geckos, Mater. Sci. Eng. C 26 (8) (2006) 1245–1250.
[43] F. Torres, O. Troncoso, J. Nakamatsu, C. Grande, C. Gomez, Characterization of the nanocomposite laminate structure occurring in fish scales from *Arapaima gigas*, Mater. Sci. Eng. C 28 (8) (2008) 1276–1283.
[44] Y. Lin, C. Wei, E. Olevsky, M.A. Meyers, Mechanical properties and the laminate structure of *Arapaima gigas* scales, J. Mech. Behav. Biomed. Mater. 4 (7) (2011) 1145–1156.
[45] A.M.C. Garrano, G. La Rosa, D. Zhang, L.-N. Niu, F. Tay, H. Majd, D. Arola, On the mechanical behavior of scales from *Cyprinus carpio*, J. Mech. Behav. Biomed. Mater. 7 (2012) 17–29.
[46] S. Gil-Duran, D. Arola, E. Ossa, Effect of chemical composition and microstructure on the mechanical behavior of fish scales from Megalops Atlanticus, J. Mech. Behav. Biomed. Mater. 56 (2016) 134–145.
[47] S. Ghods, S. Murcia, E. Ossa, D. Arola, Designed for resistance to puncture: the dynamic response of fish scales, J. Mech. Behav. Biomed. Mater. 90 (2019) 451–459.
[48] J.H. McElhaney, Dynamic response of bone and muscle tissue, J. Appl. Physiol. 21 (4) (1966) 1231–1236.
[49] R.R. Adharapurapu, F. Jiang, K.S. Vecchio, Dynamic fracture of bovine bone, Mater. Sci. Eng. C 26 (8) (2006) 1325–1332.
[50] J. McKittrick, P.-Y. Chen, L. Tombolato, E. Novitskaya, M. Trim, G. Hirata, E. Olevsky, M. Horstemeyer, M. Meyers, Energy absorbent natural materials and bioinspired design strategies: a review, Mater. Sci. Eng. C 30 (3) (2010) 331–342.

[51] R.C. Haut, R.W. Little, A constitutive equation for collagen fibers, J. Biomech. 5 (5) (1972) 423–430.
[52] M.A. Meyers, Y. Lin, E. Olevsky, P.Y. Chen, Battle in the Amazon: arapaima versus piranha, Adv. Eng Mat. 14 (5) (2012) B279–B288.
[53] W. Yang, S.E. Naleway, M.M. Porter, M.A. Meyers, J. McKittrick, The armored carapace of the boxfish, Acta Biomater. 23 (2015) 1–10.
[54] W.E. Bemis, A. Giuliano, B. McGuire, Structure, attachment, replacement and growth of teeth in bluefish, Pomatomus saltatrix (Linnaeus, 1776), a teleost with deeply socketed teeth, Zoology 108 (4) (2005) 317–327.
[55] D. Zhu, L. Szewciw, F. Vernerey, F. Barthelat, Puncture resistance of the scaled skin from striped bass: collective mechanisms and inspiration for new flexible armor designs, J. Mech. Behav. Biomed. Mater. 24 (2013) 30–40.
[56] W.C. Oliver, G.M. Pharr, An improved technique for determining hardness and elastic modulus using load and displacement sensing indentation experiments, J. Mater. Res. 7 (6) (1992) 1564–1583.
[57] K.D. Jandt, Fishing for compliance, Nat. Mater. 7 (9) (2008) 692–693.
[58] L. Wang, J. Song, C. Ortiz, M.C. Boyce, Anisotropic design of a multilayered biological exoskeleton, J. Mater. Res. 24 (12) (2009) 3477–3494.
[59] J.D. Currey, The design of mineralised hard tissues for their mechanical functions, J. Exp. Biol. 202 (23) (1999) 3285–3294.
[60] W. Yang, B. Gludovatz, E.A. Zimmermann, H.A. Bale, R.O. Ritchie, M.A. Meyers, Structure and fracture resistance of alligator gar (Atractosteus spatula) armored fish scales, Acta Biomater. 9 (4) (2013) 5876–5889.
[61] A.K. Dastjerdi, F. Barthelat, Teleost fish scales amongst the toughest collagenous materials, J. Mech. Behav. Biomed. Mater. 52 (2015) 95–107.
[62] R. Nalla, J. Kinney, R. Ritchie, Effect of orientation on the in vitro fracture toughness of dentin: the role of toughening mechanisms, Biomaterials 24 (22) (2003) 3955–3968.
[63] P. Purslow, Measurement of the fracture toughness of extensible connective tissues, J. Mater. Sci. 18 (12) (1983) 3591–3598.
[64] S. Murcia, M. McConville, G. Li, A. Ossa, D. Arola, Temperature effects on the fracture resistance of scales from Cyprinus carpio, Acta Biomater. 14 (2015) 154–163.
[65] W Yang, H Quan, MA Meyers, RO Ritchie, Arapaima fish Scale: one of the toughest flexible biological materials, Matter 6 (2019) 1557–1566.
[66] L. Wondraczek, J.C. Mauro, J. Eckert, U. Kühn, J. Horbach, J. Deubener, T. Rouxel, Towards ultrastrong glasses, Adv. Mater. 23 (2011) 4578–4586.
[67] A Wat, JI Lee, CW Ryu, B Gludovatz, J Kim, A.P. Tomsia, T. Ishikawa, J. Schmitz, A. Meyer, M. Alfreider, D. Kiener, E.S. Park, R.O. Ritchie, Bioinspired nacre-like alumina with a bulk-metallic glass-forming alloy as a compliant phase, Nat. Commun. 10 (2019) 1–12.
[68] L.J. Bonderer, A.R. Studart, L.J. Gauckler, Bioinspired design and assembly of platelet reinforced polymer films, Science 319 (2008) 1069–1073.
[69] P. Podsiadlo1, A.K. Kaushik, E.M. Arruda, A.M. Waas, B.S. Shim, J. Xu, H. Nandivada1, B.G. Pumplin, J. Lahann, A. Ramamoorthy, N.A. Kotov, Ultrastrong and stiff layered polymer nanocomposites, Science 318 (2007) 80–83.
[70] P. Walley, Y. Zhang, J.R.G. Evans, Self-assembly of montmorillonite platelets during drying, Bioinsp. Biomim. 7 (2012) 046004.
[71] H.D. Espinosa, A.L. Juster, F.J. Latourte, O.Y. Loh, D. Gregoire, P.D. Zavattieri, Tablet-level origin of toughening in abalone shells and translation to synthetic composite materials, Nat. Commun. 2 (2011) 1–9.
[72] Z Jia, Y Yu, S Hou, L Wang, Biomimetic architected materials with improved dynamic performance, J. Mech. Phy. Sol. 125 (2019) 178–197.
[73] M Mirkhalaf, AK Dastjerdi, F Barthelat, Overcoming the brittleness of glass through bio-inspiration and micro-architecture, Nat. Commun. 5 (2014) 3166.
[74] F. Bouville, E. Maire, S. Meille, B.V. d. Moortèle, A.J. Stevenson, S. Deville, Strong, tough and stiff bioinspired ceramics from brittle constituents, Nat. Mater. 13 (2014) 508 –214.
[75] L.S. Berg, in: Classification of Fishes both Recent and Fossil, JW Edwards, Ann Arbor, Michigan, 1947, p. 517.
[76] J. Long, M. Hale, M. Mchenry, M. Westneat, Functions of fish skin: flexural stiffness and steady swimming of longnose gar, *Lepisosteus osseus*, J. Exp. Biol. 199 (10) (1996) 2139–2151.
[77] H. Ehrlich, Biological Materials of Marine Origin, Springer, 2010.
[78] H. Quan, W. Yang, M. Lapeyriere, E. Schaible, R. O.Ritchie, M. A.Meyers, Structure and mechanical adaptability of a modern elasmoid fish scale from the common carp, Matter 3 (3) (2020) 842.
[79] H. Quan, W. Yang, Z. Tang, R.O. Ritchie, M.A. Meyers, Active defense mechanisms of thorny catfish, Mater. Today 38 (2020) 35.
[80] A.A.R. Browning, Mechanics and Design of Flexible Composite Fish Armor, Massachusetts Institute of Technology, 2012.
[81] J. Song, Multiscale Materials Design of Natural Exoskeletons: Fish Armor, Massachusetts Institute of Technology, 2011.
[82] R. Martini, F. Barthelat, Stability of hard plates on soft substrates and application to the design of bioinspired segmented armor, J. Mech. Phys. Solids 92 (2016) 195–209.
[83] V.R. Sherman, N.A. Yaraghi, D. Kisailus, M.A. Meyers, Microstructural and geometric influences in the protective scales of *Atractosteus spatula*, J. R. Soc. Interface 13 (125) (2016) 20160595.
[84] E.A. Zimmermann, B. Gludovatz, E. Schaible, N.K. Dave, W. Yang, M.A. Meyers, R.O. Ritchie, Mechanical adaptability of the Bouligand-type structure in natural dermal armour, Nat. Commun. 4 (1) (2013) 1–7.
[85] R. Martini, Y. Balit, F. Barthelat, A comparative study of bio-inspired protective scales using 3D printing and mechanical testing, Acta Biomater. 55 (2017) 360–372.
[86] S. Rudykh, C. Ortiz, M.C. Boyce, Flexibility and protection by design: imbricated hybrid microstructures of bio-inspired armor, Soft Matter. 11 (13) (2015) 2547–2554.
[87] N. Funk, M. Vera, L.J. Szewciw, F. Barthelat, M.P. Stoykovich, F.J. Vernerey, Bioinspired fabrication and characterization of a synthetic fish skin for the protection of soft materials, ACS Appl. Mater. Inter. 7 (10) (2015) 5972–5983.
[88] R. Martini, F. Barthelat, Stretch-and-release fabrication, testing and optimization of a flexible ceramic armor inspired from fish scales, Bioinspir. Biomim. 11 (6) (2016) 066001.
[89] E. Lin, Y. Li, C. Ortiz, M.C. Boyce, 3D printed, bio-inspired prototypes and analytical models for structured suture interfaces with geometrically-tuned deformation and failure behavior, J. Mech. Phys. Solids 73 (2014) 166–182.
[90] L. Szewciw, D. Zhu, F. Barthelat, The nonlinear flexural response of a whole teleost fish: contribution of scales and skin, J. Mech. Behav. Biomed. Mater. 76 (2017) 97–103.
[91] J. Duro-Royo, K. Zolotovsky, L. Mogas-Soldevila, S. Varshney, N. Oxman, M.C. Boyce, C. Ortiz, MetaMesh: a hierarchical computational model for design and fabrication of biomimetic armored surfaces, Comput. Aided Des. 60 (2015) 14–27.
[92] P. Liu, D. Zhu, Y. Yao, J. Wang, T.Q. Bui, Numerical simulation of ballistic impact behavior of bio-inspired scale-like protection system, Mater. Des. 99 (2016) 201–210.
[93] C. Zhang, P. Rawat, P. Liu, D. Zhu, A new design and performance optimization of bio-inspired flexible protective equipment, Bioinspir. Biomim. 15 (2020) 066003.
[94] R. Ghosh, H. Ebrahimi, A. Vaziri, Contact kinematics of biomimetic scales, Appl. Phys. Lett. 105 (23) (2014) 233701.